Anthropogenic Heat of Power Generation in Singapore: analyzing today and a future electromobility scenario

DELIVERABLE TECHNICAL REPORT

Version 1 - 30/04/2020

D 1.2.2.3 – Anthropogenic Heat of Power Generation in Singapore: analyzing today and a future electromobility scenario

Project ID	NRF2019VSG-UCD-001
Project Title	**Cooling Singapore 1.5:** **Virtual Singapore Urban Climate Design**
Work Package ID	WP1.2. Environmental assessment report
Deliverable ID	D1.2.2.3 – Power plant heat module
Authors	David Kayanan, Jimeno A. Fonseca, Leslie Norford
Date of Report	30/04/2020
DOI	10.3929/ethz-b-000412794

Version	Date	Modifications	Reviewed by:
-	07/03/2020	First draft	Jimeno A. Fonseca, Leslie Norford
1	30/04/2020	Revisions; included waste heat streams	Jimeno A. Fonseca

(SEC) SINGAPORE-ETH CENTRE 新加坡-ETH 研究中心 SMART TUMCREATE NUS National University of Singapore Agency for Science, Technology and Research

ABSTRACT

This report studies the anthropogenic heat emissions of Singapore's power generation sector and evaluates the potential future emissions with electromobility across the island. We thus developed a power plant dispatch model to downscale the total heat released by the power sector in 2016. Taking electricity demand and fuel prices as inputs, the model was based on an energy-only model of the National Electricity Market of Singapore. Generation companies were assumed to bid at marginal cost and discount the value of cogeneration heat. This led to a higher correlation of electricity prices and demand than in reality, and sensitivity to fuel prices. The model is capable of calculating the dispatch, fuel consumption, cogeneration heat and waste heat streams of each plant. These heat profiles would then serve as inputs to a WRF mesoscale model of Singapore.

The model was calibrated with the monthly fuel mix and annual fuel consumption in 2016 via hyperparameter optimization. An RMSE of 4.67 ktoe was achieved in the electricity produced per month and per fuel, and the total released heat was within 1.88% of the energy statistics. Simulation of the baseline electricity demand showed that CCGT PNG plants emit over half of the waste heat (1796 ktoe of 3282 ktoe), with the Senoko power plant releasing half of this. Cogeneration CCGT plants released about 882 ktoe of waste heat, while producing as much as 1813 ktoe of process heat. As much as 47% of the total waste heat is released into the air as sensible heat, and 27% as latent heat, with the rest released into the sea.

Based on data from a previous study on the anthropogenic heat emissions in the transportation sector, we simulated a scenario wherein the road transportation in Singapore was fully electrified. This scenario could have an additional waste heat of 248 ktoe, and an additional electricity demand of 369 ktoe. This additional demand represents a reduction of vehicle heat on the roads by a factor of six, and more heat is emitted at far-away and efficient cogeneration plants. Overall, the estimated reduction in total anthropogenic heat is 1473 ktoe, or about 7% less than in 2016.

Table of Contents

Nomenclature

Subscripts

e	Electricity
q	Cogeneration useful heat
$fuel$	Arbitrary fuel for power generation

Quantities

Output, Efficiencies and Costs

P_o	Generating unit output $[MW_e]$
Q_{cogen}	Cogeneration output heat $[MWh_q]$
η_e	Electrical efficiency $[\frac{MWh_e}{MWh_{fuel}}]$
$\eta_{e\,FL}$	Full-load electrical efficiency $[\frac{MWh_e}{MWh_{fuel}}]$
η_q	Cogeneration useful heat efficiency $[\frac{MWh_q}{MWh_{fuel}}]$
η_{total}	Cogeneration full load power and heat efficiency $[\frac{MWh_{e+q}}{MWh_{fuel}}]$
HPR	Cogeneration heat-to-power ratio $[\frac{MWh_q}{MWh_e}]$
η_{boiler}	Thermal efficiency of a fictitious boiler, as an alternative to cogeneration heat $[\frac{MWh_q}{MWh_{fuel}}]$
$Price_{fuel}$	Fuel price in S$ per original fuel denomination $[\frac{S\$}{fuel\ units}]$
$conversion_{\,fuel}$	Fuel conversion factor to per MWh_{fuel} $[\frac{fuel\ units}{MWh_{fuel}}]$

Reliability

T	Online duration random variable $[market\ period]$
D	Downtime duration random variable $[market\ period]$
S_0	Starting state random variable [-]
λ	Failure rate. Exponential parameter of the time to fail. $[market\ period^{-1}]$
μ	Repair rate. Exponential parameter of the time to repair. $[market\ period^{-1}]$
$MTTF$	Meant time to fail $[market\ period]$ or $[week]$
$MTTR$	Meant time to repair $[market\ period]$ or $[week]$
A_{lim}	Limiting availability [-]
AF	Average failures$[week^{-1}]$ or $[yr^{-1}]$

Acronyms and Abbreviations

AH	Anthropogenic Heat
WRF	Weather Research and Forecasting
HHV	Higher heating value
LHV	Lower heating value
CCGT	Combined-Cycle Gas Turbine
OCGT	Open-Cycle Gas Turbine
ST	Steam Turbine
WtE	Waste-to-Energy
cogen	Cogeneration
PNG	Piped natural gas
LNG	Liquefied natural gas
NEMS	National Electricity Market of Singapore
USEP	Uniform Singapore Electricity Price

1 Introduction

This technical report studies the anthropogenic heat emissions of Singapore's power generation sector and evaluates its potential future emissions with electromobility (e-mobility) across the island. This report is part of the Cooling Singapore (CS) project, which aims to study urban warming in tropical Singapore. It also explores and assesses strategies that could mitigate the warming or allow its citizens to adapt to it. In the first version of CS (CS1.0), the Urban Heat Island (UHI) effect was simulated at the mesoscale for the whole island of Singapore using a Weather Research and Forecasting (WRF) model (Mughal, et al., 2019). However, this incorporated a coarse modeling of anthropogenic heat (AH), which is one of the drivers of urban warming and the UHI. In the current phase of the CS project (CS 1.5), we improve the mesoscale analysis by incorporating detailed models of AH in the WRF model. A preliminary study of these AH sources across Singapore was done in (Kayanan, Resende Santos, Ivanchev, Fonseca, & Norford, 2019). A following study focused on AH in road transportation (Ivanchev & Fonseca, 2020). This third technical report focuses on the modeling of the AH from the power sector.

1.1 Objectives

The objectives of this report include:

1. Develop a model that calculates spatiotemporal heat profiles of Singapore's power sector, specifically from its power plants. These profiles, which will serve as **inputs to the WRF mesoscale model** of CS 1.5, must be specified as per:

    a. Location, i.e. in which 300 m-by-300 m WRF grid cell the heat is emitted
    b. Time, given at least in the hourly resolution
    c. Component heat streams; specifically, as sensible heat into the air, latent heat into the air, and heat released into the sea.

2. Calibrate the model with the yearly heat released by the power sector of Singapore (Kayanan, Resende Santos, Ivanchev, Fonseca, & Norford, 2019).

3. Use the model to estimate the potential heat release of the power sector under multiple scenarios of demand (e.g. full electrification of road transport).

1.2 Power plant dispatch is key to modeling the heat from the power sector

Power plants, specifically thermal power plants, are the principal source of heat in the power sector. These plants can have different production profiles, but can also have no output due to circumstances such as plant outages and grid congestion. Thus, to model the heat from the power sector in both space and time, we must first understand *how* the power plants are dispatched in Singapore.

Let's suppose that we have some knowledge of the power plant dispatch. We can estimate the heat that is released by power-only, thermal stations by noting that any amount of fuel not converted into electricity ends up as some form of heat.

$$Fuel\ HHV(t) = \ Net\ Electricity(t) + \ Released\ Heat(t) \tag{1}$$

In Eq. (1), we define the heat released as the difference between the higher heating value (HHV) of the consumed fuel and the net electricity produced. This heat is released as various streams discussed in Section 1.3. By ignoring any warm-up and cool-down processes, this relationship can be alternatively expressed via the electrical efficiency η_e in Eq. (2).

$$Released\ Heat(t) = \ Net\ Electricity(t)(\frac{1}{\eta_e} - 1) \tag{2}$$

The overall problem thus consists of two parts: 1) modelling the power plant dispatch; and 2) modelling the internal energy flows and heat release given the production schedules as in Eq. (2).

In Singapore, the power plants are dispatched via a liberalized electricity market, the National Electricity Market of Singapore (NEMS). Given the available data and information, we chose to model the bidding of generator companies in an energy-only NEMS model under the assumption of a perfectly competitive market. This is formally stated in Section 2.2.

1.3 Heat from power plants

There are different types of electricity generation technologies such as fossil fuel-based generation, nuclear energy, hydropower and so on. One major class is *thermal* power generation, and the **Singaporean power plant fleet is virtually thermal**. About 95% of its electricity was generated from natural gas via combined cycle gas turbine (CCGT) plants from 2014-2018 (Energy Market Authority, 2018).

Thermal power generation mostly involves the combustion of fuels, but also includes nuclear fission, geothermal energy, and solar thermal energy. These energy sources release thermal energy or heat which can only be partially converted into electricity, as governed by the 2nd Law of Thermodynamics. Table 1 lists major types of thermal power plants and efficiencies as measured in a sample of stations in the US. The heat released by thermal stations is composed of this unconverted heat, as well as any electricity consumed by the station itself to run auxiliary equipment, which ultimately turns into heat. These various waste heat streams can be classified as:

1. *stack heat* – heat retained in the combustion products, the majority of which exit as flue gases, but can also be retained in ashes as in the case of coal. These hot gasses carry sensible heat as well as the latent heat absorbed by any existing moisture in the fuel and the water product of combustion.

2. *heat rejected by condenser* – heat released by the working fluid in the condensation step of Rankine cycles (e.g. steam cycle in coal and CCGT power plants). This heat can be released via the major types of cooling systems in Table 2.

3. *miscellaneous losses and heat from own electricity consumption* – minor heat losses in a power plant. Miscellaneous losses include radiation form hot surfaces (e.g. of boilers) and mechanical and electrical losses, typically not more than 1% of the fuel input. The electricity that power plants use to run its auxiliary processes also diffuses as heat, which is typically 5% to 8% of the input fuel (Chen, et al., 2010) (Noordermeer) .

Furthermore, cogeneration plants (*aka* combined heat and power, or CHP) also produce process heat for nearby industrial customers or on-site processes. As an end-use product, it must be attributed to industry and not as waste heat released by power plants (Kayanan, Resende Santos, Ivanchev, Fonseca, & Norford, 2019). In Singapore, Jurong island is the site of most utility cogeneration stations, which serve the heat demands of the refining, petrochemicals and specialty chemicals industries in a strategic, shared-utilities complex (JTC, 2020).

Table 1 Thermal power plants and measured full load HHV efficiencies in the US in 2008-2018 (US Energy Information Administration, 2019)

Thermal power plant	**Full Load HHV Efficiency** *weighted by Net Summer Capacity*
CCGT (natural gas)	44.5% - 44.8%
OCGT (natural gas)	29.4% - 30.6%
Coal-fired ST	33.6% - 34.1%
Oil-fired ST	32.8% - 33.6%
Nuclear plant	32.5% - 32.6%

Table 2 Major cooling systems of thermal power plants

Cooling Technology	Operating Principle	Heat released as
Once-through	A flow from a nearby body of water (e.g. river, sea) is redirected into the plant to draw the unconverted heat in the working fluid. This cooling system uses the most amount of water.	Heated water merging with the natural source (sensible heat in water)
Wet-recirculating	Use of a cooling water loop: 1. Heat is drawn from condensing the working fluid to the cooling fluid 2. Partial evaporation of cooling fluid to reject the heat Because of partial evaporation, only part of the cooling liquid flow has to be replenished, leading to less water consumption.	Steam billowing from wet cooling towers (sensible and latent heat in humid air)
Dry-cooling	Use of air for cooling, which drastically reduces water consumption but impairs thermal efficiency.	Heated air escaping from dry cooling towers (sensible heat in air)

In accounting the energy flows in a thermal power plant, the energy content of its fuel is an important consideration. The heat released in the combustion of fuels is defined by the higher heating value (HHV) and the lower heating value (LHV) (Bossel, 2003). The difference of the two lies in the final state of the combustion products. The HHV is measured until the products return to 25 °C and thus releases the latent heat of vaporization of water in the products and any pre-existing moisture. Whereas, the LHV is defined only until the products return to 150 °C, excluding their additional sensible and latent heat.

Heat engines are typically designed to have exhaust temperatures well above the saturation temperature of water (e.g. around 150 °C for boilers, and 400 °C to 650 °C for gas turbines (Noordermeer)), which means that the latent heat of combustion is released into the environment via the stack.

These energy flows and their proportions are portrayed in Sankey diagrams for a coal power plant and a CCGT plant in Figure 1, which shows how the heat exiting the stack and condenser compare to each other given different power plant technologies.

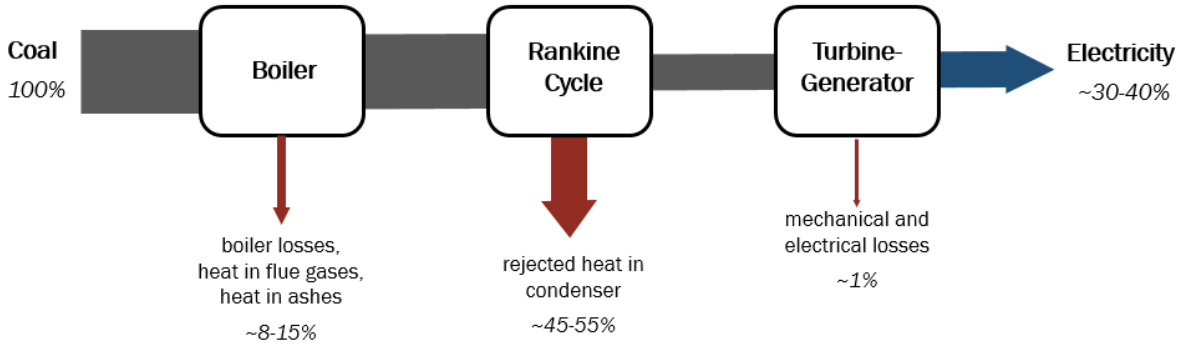

(a) Coal power plant. Adapted (Suresh, Reddy, & Kolar, 2012) (Erdem, et al., 2010)

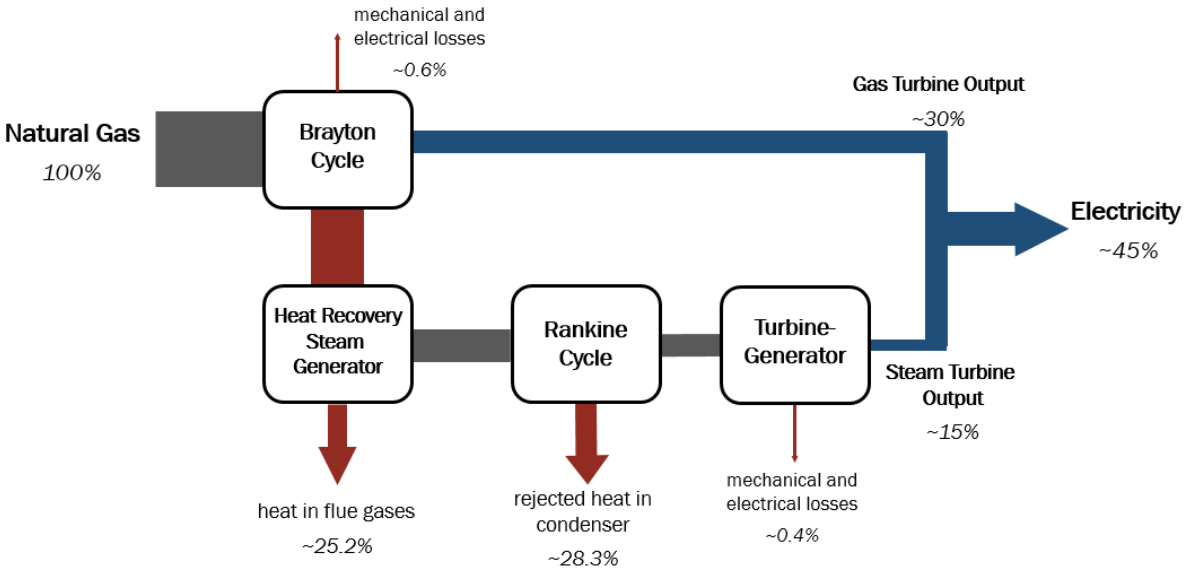

(b) CCGT power plant. Adapted (Nag, 2002)

Figure 1 Energy flows and heat losses in thermal power plants

As can be seen in the AH Sankey diagram (Kayanan, Resende Santos, Ivanchev, Fonseca, & Norford, 2019) and summarized in Table 3, most of the heat from the power sector is generated by the power plants. Only a limited amount is released in the transmission and distribution of electricity, and is further discussed in Section1.4. An upper bound of the cogeneration heat was also estimated.

Table 3 Power sector heat estimate in 2016 (Kayanan, Resende Santos, Ivanchev, Fonseca, & Norford, 2019)

Heat Source	2016 estimate in ktoe
Power plants	5099*
Power grid	255

**Up to 2235 ktoe as cogeneration heat*

A database of the power stations containing basic technical information was built and can be found in Annex A. Figure 2 below shows a map of these stations with capacity and fuel information.

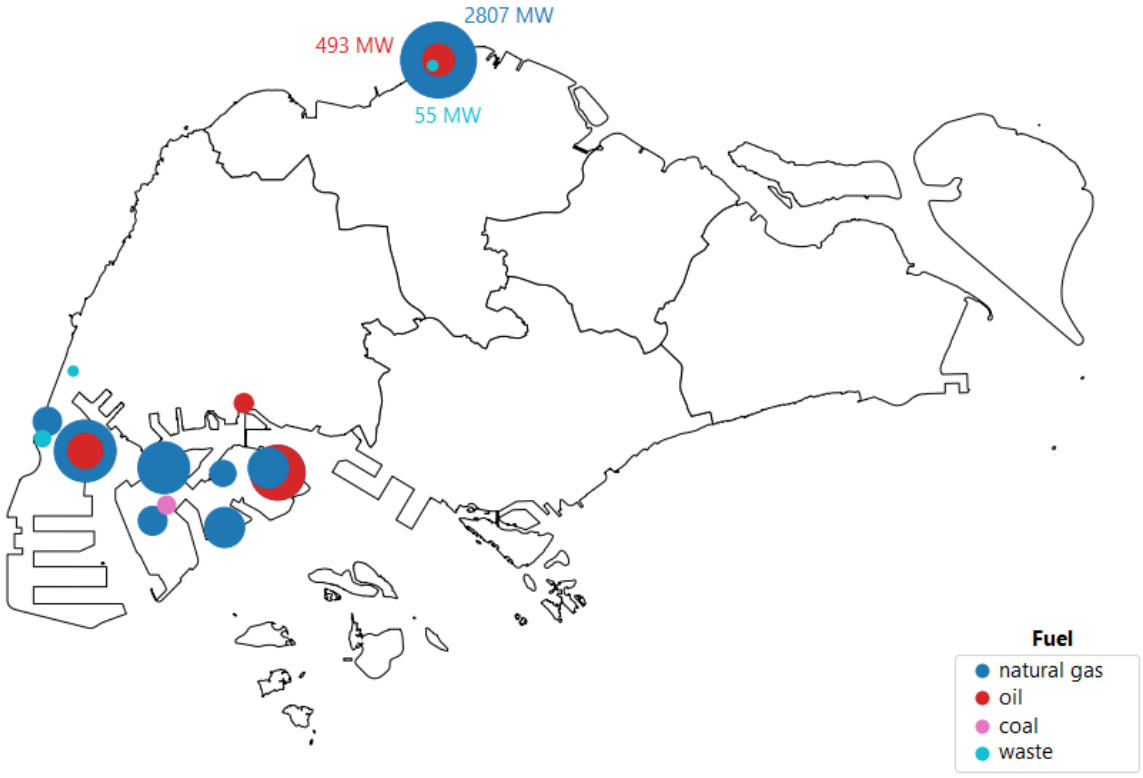

Figure 2 Singapore power plant locations and capacities by fuel

**Size is to MW capacity*

1.4 Heat from the power grid

The power grid generates heat via resistance losses in lines and electromagnetic losses in transformers, switchgear and other power conditioning equipment. These losses include both:

- active power losses, which is traded energy lost in transmission; and
- reactive power losses, which is not traded energy but instead a grid requirement to maintain acceptable power quality.

Singapore's power grid was able to deliver an estimated **4181 ktoe** out of the **4436 ktoe** of power generated, or an overall efficiency of **94.3%** (Energy Market Authority, 2018). Furthermore, whereas power plants are point sources of heat in the mesoscale, the power grid is a more distributed infrastructure located entirely underground in Singapore (SP Group, 2017). Thus, the impacts of the heat from the grid to urban warming is expected to be negligible.

1.5 National Electricity Market of Singapore

Singapore operates a liberalized wholesale electricity spot market, the National Electricity Market of Singapore (NEMS). An overview of the industry structure and its stakeholders is provided in (Energy Market Authority, 2010), and additional resources include (Energy Market Company, 2018) (Feiyu Lu & Gan, 2008) (Gao, Zhou, Shu, & Beng, 2017). As the platform for meeting Singapore's electricity demand in real time, this market environment determines the generator dispatch, and procures multiple products and not just energy, as summarized in Table 4.

Although electrical energy quoted in MWh is the main product, two additional products, regulation and reserves, are necessary to ensure a stable and reliable operation of the power system, in the face of non-ideal conditions and contingencies. NEMS co-optimizes these three products, with the primary objective of minimizing energy costs and promoting efficiency and competition in the market.

For the purposes of heat modeling, determining the energy dispatch is required at the minimum. The regulation product is continuously acting but is noise-like. The reserve product is only used in contingencies and expected to contribute little energy over the span of a year.

Table 4 Products traded in the NEMS

Product	Description and Usage	Dynamics and Heat Characteristic
Energy	Energy production to meet the demand. Supply and demand must be balanced at all times, and this product matches the aggregate consumption behavior of the system as it various throughout the day. The generator energy dispatch is considered the planned, normal operating schedule of the system.	• Steady energy production and therefore heat generation. • Follows changes in the aggregate load throughout the day, defined in 30-min periods.
Regulation*	In contrast to energy, this service matches supply and demand in a much finer temporal scale and magnitude: • minute and sub-minute scale; • minor fluctuations and noise in the demand, respectively. The market determines the *capacity* (MW) that generators must have available to provide this; the actual output adjustment is controlled by governor systems to maintain the system frequency. Thus, the net energy (MWh) and heat are determined only after the fact. In NEMS, regulation is considered as not necessarily energy-zero, and activated generators are compensated/billed for the energy surplus/deficit incurred when providing this service.	• Minor power fluctuations on top of the scheduled output[1], acting *continuously*. • The net energy and heat are determined only after the fact.

[1] Power plants need to offer energy before they can offer regulation. This is because power plants have a minimum stable output level, and this offered capacity is used without any intended delays and continuously.

Table 4 Products traded in the NEMS (continued)

Product	Description and Usage	Dynamics and Heat Characteristic
Reserve*	This service is activated upon system contingencies, wherein system disruptions (in the generators, the grid or the loads) cause significant imbalance in the system, threatening the system stability. As a contingency service, its activation is independent of the market mechanism or the load.	• Chance activation upon system contingencies. • Standby capacity on top of schedule output[2]. • Upon activation, reserves are expected to hold their output as advised by the power system operator.

**In the United States and in Europe, Primary Frequency Response is the equivalent of NEMS' regulation service, and Secondary and Tertiary Frequency Response are equivalent to the reserve service. This is not to be confused with the three classes of reserves in the NEMS (i.e. primary, secondary and tertiary).*

[2] Three reserve classes are defined (primary, secondary and tertiary), which specify a response time of the generators. In principle, the power plant need not be online as long as it makes the response time, but thermal plants cannot meet this limit unless they are online.

2 Methodology

2.1 Methodological Framework

The methodology can be summarized as following, and the following sections describe each of these phases:

1. *Problem formulation*

   The modeling approach and assumptions were made based on the limited available data on the power sector and the stated objectives.

2. *Data collection*

   The following data in 2016 were acquired:

   a) Database of Singapore's power plant, including their fuel, generation and cooling systems

   b) energy market data
      - Market fundamentals that explain the economics of power generation (e.g. fuel prices, demand data). These define the baseline.
      - Electricity generation statistics, which describe the dispatch and can be used to calibrate the results.

3. *NEMS modeling*

   An energy-only model of the NEMS was developed, which describes the dispatch of power plants under normal power grid conditions.

4. *Power plant modeling*

   The power plant production costs were estimated and their bidding behavior modelled. Internal energy flows were modelled to calculate the waste heat streams. Plant outages were also modeled.

5. *Baseline calibration*

   The unknown efficiency and reliability plant parameters were calibrated to fit the 2016 generation statistics.

6. *Scenario simulation and calculation of the input heat streams for WRF*

   The 2016 baseline and the full electrification of road transport scenario were simulated, and the waste heat streams of April were processed as inputs for WRF.

2.2 Problem Formulation

We formalize the problem as follows:

Calculate	Waste and cogeneration heat of Singapore's power plants, per station and in a 30-min resolution (NEMS market period)
Assumptions	1. The power plants are dispatched via merit order in an energy-only market. We further neglect any real-time deviations from the dispatch. 2. The market is *perfectly competitive*, and interactions with other markets (e.g. electricity futures) can be neglected. Thus, generator companies bid at marginal cost, defined by their fuel costs.
Inputs	Electricity market fundamentals: • system demand forecast • fuel prices (or proxies) Power plant data: • generation technology and fuel used • technical parameters (e.g. capacity, efficiencies) • reliability parameters • fuel heating values
Such that	The model is calibrated until the power plant dispatch matches the following statistics, in decreasing priority: 1. Monthly electricity production by fuel (Table 7) 2. Annual fuel consumption (Table 8) 3. Approximate limits – LNG imports, cogeneration heat Furthermore, the total heat released by all power plants must be reasonably close to the estimate.

We built an energy-only model of the NEMS because the energy dispatch of power plants accounts for almost all of the energy flows and makes the complexity appropriate for heat modelling. Assuming that generator companies bid at marginal cost is necessary owing to

the unavailability of bid data to model actual strategic bidding. Thus, the model would reflect nothing more than the pure economics of power generation, and the calculated prices are not to be taken as predictions of the USEP.

2.3 Data Collection

a) Power plant data

The power plants in Singapore were identified from the generator licensees in (Energy Market Company, 2018) and the registered capacity in (Energy Market Authority, 2018). Table 5 summarizes the information necessary to model the power plants. The information was collated from company websites and other sources available in the public domain.

Table 5 Information on power plants

Feature	Notes
Generating units	Generating units per power plant, categorized by prime mover technology and fuel
Registered capacity	Used as maximum output power. The registered capacity is typically derated from the nameplate capacity.
Minimum stable generation	No data was available, so this was assumed to be half of the capacity.
Prime mover*	Turbine technology, as well as cogeneration
Fuel*	Primary fuel
Full load electrical efficiency	Not available anywhere, so this had to be calibrated.
Part-load performance	These curves were obtained from samples in (PA Consulting Group, 2018) (Strbac & Aunedi, 2016) and assigned randomly.
Full load heat and power efficiency (cogeneration)	Also not available, but this was set to the maximum values in (Bhatia, 2014).

*As discussed in *Costs and Bidding* of Section 2.5, these divide the fleet into power plant classes. Also see Table 10.

Table 5 (continued)

Feature	Notes
Internal energy flows per unit HHV fuel	These are the parameters that define the flow of the input fuel into the power plant processes and exit as electricity, cogeneration heat (if present) and waste heat streams as in Figure 1. These parameters are defined by the calibrated electrical efficiency (and the heat and power efficiency, for cogeneration) as well as typical values obtained from the sources referenced in Figure 1.
Cooling system	One of the types listed in Table 2, this was based on the presence of large hyperbolic cooling towers from satellite images of Google Maps. The lack thereof would default in the assigning once-through systems. On the other hand, WtE plants have dry-cooling systems (National Environment Agency, 2020).
Stack height	Stack heights of 100 m were assumed by default, in accordance with the typical CCGT and small coal plant stack heights in (International Finance Corportation, 2008). WtE plants have stack height info in (National Environment Agency, 2020).
Reliability parameters	Outage data are available (https://www.emcsg.com/data), but were not accessed in this project. Thus, the stochastic outages model was based on related statistics. A lower bound for A_{lim} was estimated from the generator outage capacity in (Energy Market Authority, 2019). This was obtained from the remaining capacity divided by total capacity, averaged over the available data. No other data was obtained, so the full set of parameters had to be calibrated.
Location	The station locations were set the location of the flue stacks found via Google Maps.

b) Fuel prices and heating values

Fuel price data was not available in Singapore[3], and thus the fuel commodity prices reported in (World Bank Group, 2019) were used as a proxy. For oil-fired plants that use heavy fuel oils or diesel, the price of crude was used as a proxy. The data had a monthly resolution, but daily spot price data for US natural gas (Henry Hub) was available (US Energy Information Administration, 2020). The available fuel data is summarized in Table 6. As fuel prices are

[3] We attempted to engage the Energy Market Authority for power market data in October 2019, but our request was not granted.

quoted in US dollars, weekly USD-SGD rates of 2016 were applied (Monetary Authority of Singapore, 2019).

Actual heating values were not available and were based on (Pacific Northwest National Laboratory, n.d.) (Coal Marketing International Ltd, 2020) (Energy Information Administration, 2007) (Komilis, Kissas, & Symeonidis, 2013).

Table 6 Fuel price data

Fuel	Specification	Units	Resolution
Piped Natural Gas	Henry Hub (USA)	USD/mmBTU	daily
Liquefied Natural Gas	Japan	USD/mmBTU	monthly
Petroleum products (heavy fuel oil, diesel)	Crude (Dubai), Crude (Brent), Crude (WTI)[4]	USD/bbl	monthly
Coal	Australia	USD/ton	monthly

c) Demand data

The NEMS is cleared for every half-hour period, based on forecasted data (Energy Market Corporation, 2019). To produce the baseline demand, the available demand forecast was scaled by the monthly gross electricity generation in (Energy Market Authority, 2019), as to match the actual energy flows. The final demand is shown in Figure 3.

[4] The crude prices were assigned randomly to the oil-fired plants.

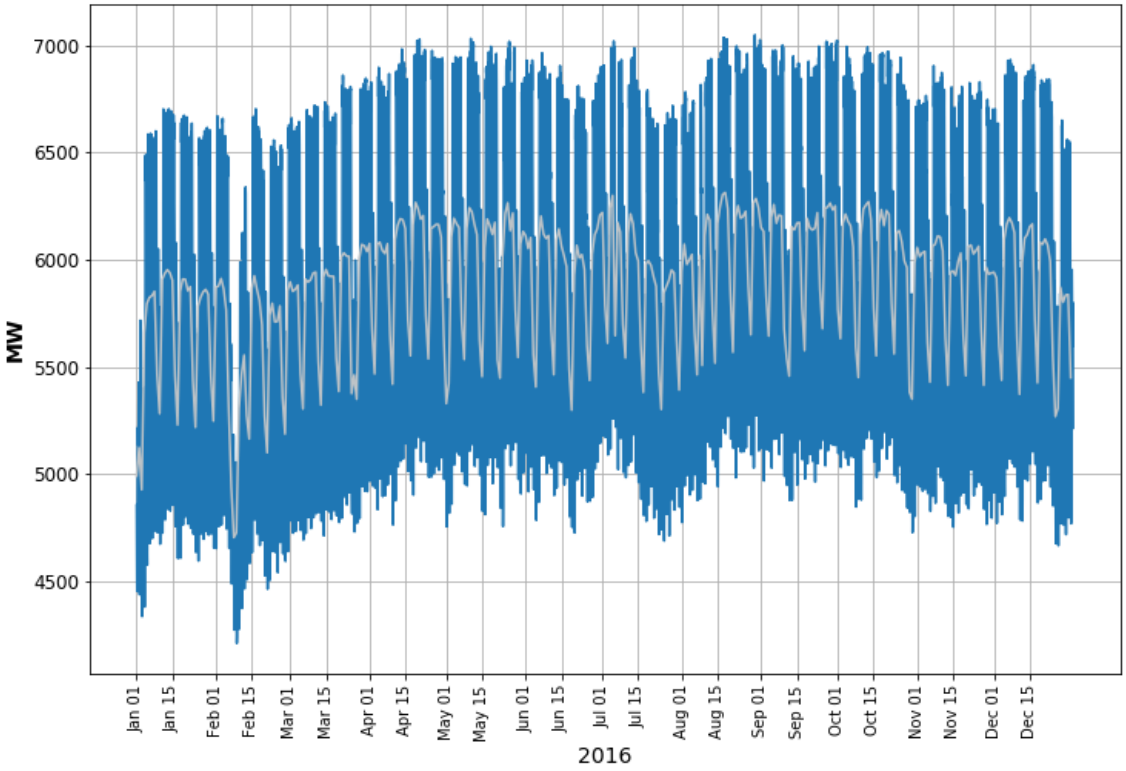

Peak demand	*7049.7 MW*
Baseload demand	*4209.3 MW*
Total demand	*4436 ktoe*

Figure 3 System demand. Daily average overlaid

d) Calibration data

Two datasets that can be used to calibrate the model were available in the Singapore Energy Statistics (SES) (Energy Market Authority, 2018):

1. Fuel mix by output electricity, per month and per major fuel category (Table 2.1)

2. Fuel mix by input fuel, annual and per major fuel category (Table 2.2.1)

These two datasets are the closest datasets to the actual dispatch, despite having a low time resolution and aggregated amongst power plants. Because the fuel mix dataset was given in terms of percentages, it was slightly processed via:

1. Correcting the rounding error. The excess/deficit percentage points were added to natural gas, because it was the largest source and thus would introduce the least relative change.

2. Convert the percentages into ktoe by scaling it with the monthly total from the demand data.

These data sets are summarized in Table 7 and Table 8.

Table 7 Fuel mix by output electricity (adapted (Energy Market Authority, 2018))

2016	**Gross electricity produced [ktoe]**			
	Natural Gas	Petroleum Products	Coal	Others
Jan	345.57	0.36	3.61	11.56
Feb	315.08	0.99	3.64	11.25
Mar	354.17	0.74	4.82	11.13
Apr	354.20	0.74	4.81	10.36
May	363.86	0.76	5.33	11.05
Jun	350.67	0.37	5.13	10.26
Jul	358.89	1.50	4.88	10.14
Aug	370.32	1.92	2.69	10.01
Sep	352.38	3.74	5.23	12.33
Oct	364.57	0.76	5.34	11.07
Nov	335.94	14.23	4.74	9.85
Dec	354.78	3.75	4.87	11.24

Table 8 Fuel consumption in 2016 (Energy Market Authority, 2018)

Fuel	**Consumption [ktoe]**
Natural Gas	8364.23
Petroleum Products	122.80
Coal	259.22
Others	788.60

2.4 NEMS Modeling

As explained in Section 1.5, the NEMS is simplified as an energy-only market to reduce modeling complexity. The energy-only market rules are summarized in Table 9**.**

Table 9 Rules of the simplified NEMS model

Market Period	• Half-hour duration • Periods are independent; the NEMS is a self-commitment market (Feiyu Lu & Gan, 2008)[5]
Offer bids	• Only half-hourly bids, which can be wholly rejected, partially- or fully-accepted[6]. • Participants can submit up to 10 bids per period. • Bids, given in (MW, S$/MWh), must be increasing in price. • No price limits are enforced. Negative prices are allowed.
Demand	• The half-hourly system demand is forecasted by the market operator, and serves as a model input. • The demand is price-inelastic.
Clearing	• Merit-order dispatch – the bids are sorted in increasing price. • The marginal bid, whose additional output meets the given demand, sets the price. All bids cheaper than this are accepted; conversely, all bids more expensive than this are rejected. • No transmission constraints are imposed. The market is cleared at a single price.

Because of the simple market rules, the clearing algorithm iterates through the market periods of the simulation duration (see Algorithm 1). We ask the reader to note that this algorithm is linked to the power plant model of Section 2.5.

[5] In the actual NEMS, generator companies are expected to reflect startup costs and ramping limitations in their bidding strategies.
[6] Because bids can be partially accepted (i.e. the marginal bid is generally partially accepted), it is possible that a generator is dispatched less than its minimum stable generation. This occasionally happens, but no additional measures were taken.

Algorithm 1 Market clearing

1. **Pre-simulation**
    a. Determine the half-hourly full-load efficiency of the generator units.
    b. Determine the online/offline status of the units

2. **Simulation**
    a. For each day, determine the fuel price.

    b. For each period,
        i. Calculate the bids of the online units.
        ii. Aggregate the bids in increasing bid price, calculating the accumulated supply. This is the supply curve.
        iii. Locate the marginal bid, which meets the demand for that period. Partially accept the marginal bid, until demand and supply are balanced.
        iv. Fully accept all cheaper bids. Reject the rest of the bids.
        v. Resolve the bid acceptance into the generator output, P_o
        vi. Calculate the achieved electrical efficiency, and Q_{cogen} of cogeneration plants

3. **Post-simulation**
    a. Calculate dispatch statistics

    b. Calculate fuel consumption and waste heat

Figure 4 shows the flow chart of the market simulator, indicating the relationships of the components and the flow of data. Power plants are modelled at the generating unit level, and classified by their prime mover and their fuel, which are the primary indicators of production costs. For every half-hour market period, all online generating units submit bids, and the market model decides which bids to accept such that the total costs for that period are minimized.

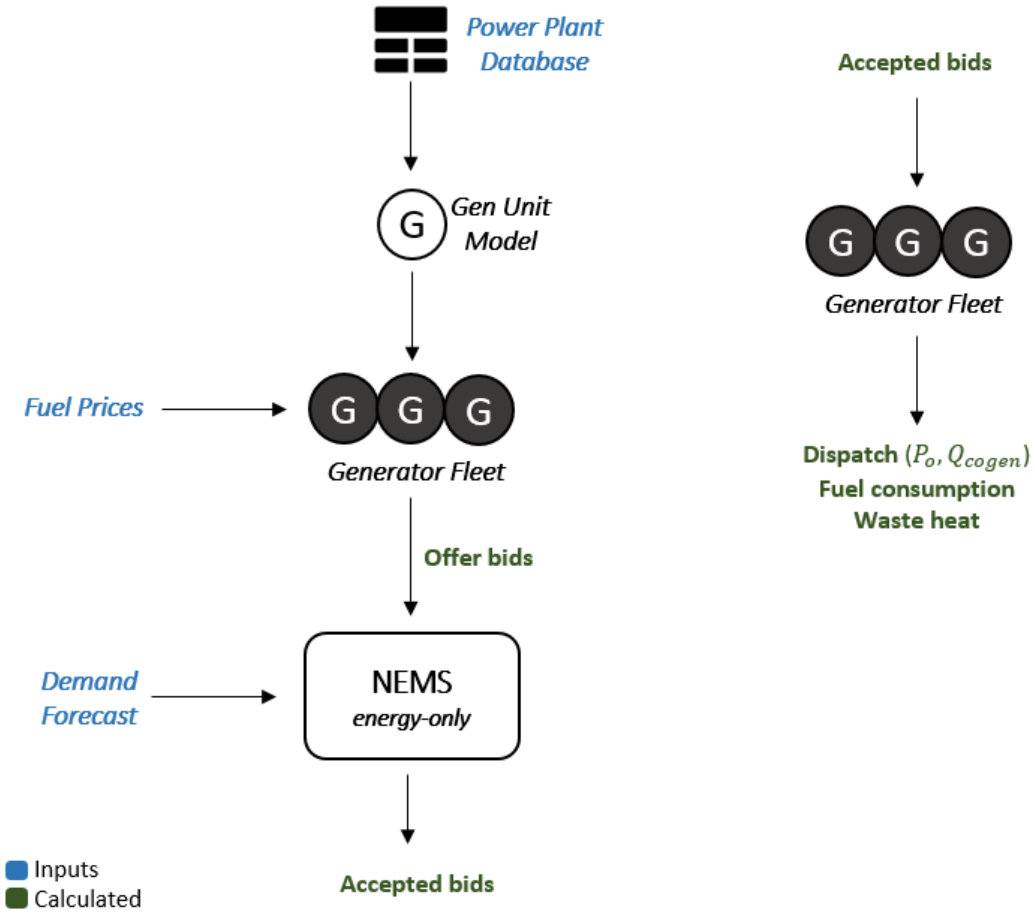

Figure 4 NEMS model flow chart

2.5 Power Plant Modeling

a) Costs and Bidding

Power plants are modelled at the generating unit level, because power plants can have multiple units, possibly running different technology-fuel combinations. These technology-fuel combinations are referred to here as *power plant classes*. The existing classes in Singapore's fleet are summarized in Table 10.

Table 10 Singapore power plant classes

Based on the power plant database in Annex A

Power Plant Class	No. Units	Total Capacity [MW]
CCGT PNG	6	4147
CCGT LNG	3	2058
Cogen CCGT PNG	2	1255
Cogen CCGT LNG	5	2721
Cogen ST Coal	1	160
ST Oil*	5	2721
Waste-to-Energy	4	204

**Oil refers to all petroleum products used as fuel for power generation, such as heavy fuel oil and diesel.*

Given that a) fuel costs dominate the production costs of fossil-based plants; and b) cogeneration plants have process heat as a secondary product, we implemented the following bidding behaviors:

1. Fossil-based, power-only bidding
2. Fossil-based, cogeneration bidding
3. Waste-to-energy bidding

1. Bidding of fossil-based, power-only plants

Production costs can be separated in terms of fixed and variable costs, as shown in Eq. (3). In calculating the marginal costs, only the variable costs have to be modelled as shown in Eq. (4)

$$Total\ Costs = Fixed\ Costs + Variable\ Costs \quad (3)$$

$$Short\text{-}Run\ Marginal\ Costs = \frac{d(Total\ Costs)}{dQ} \quad (4)$$

$$= \frac{d(Variable\ Costs)}{dQ}$$

where Q stands for output quantity; in this case the output power P_o in MW. For fossil-based power plants, the variable costs can be simplified to the dominant cost as in Eq. (5).

$$Variable\ Costs \approx Fuel\ costs \quad (5)$$
$$= Price_{fuel} \cdot conversion_{fuel} \cdot \frac{1}{\eta_e(P_o)} \cdot P_o \ \ [\text{S\$/h}]$$

The fuel price $Price_{fuel}$ was obtained from the same day, based on the available price data (We refer the reader to Section 2.3 *Data Collection*). Thus, the *discrete* short-run marginal costs, or $SRMC$, between a bid defined from output level P_{lb} to P_{ub} is given by

$$SRMC(P_{lb}, P_{ub}) = Price_{fuel} \cdot conversion_{fuel} \cdot \frac{\Delta}{\Delta P_o}\left(\frac{1}{\eta_e(P_o)} \cdot P_o\right)\Big|_{P_{lb}}^{P_{ub}} \quad (6)$$

where P_{lb}, P_{ub} denote the lower and upper bounds of the bid, respectively. We then explain some of the details of this calculation.

a) Fuel denominations and conversion factors

As shown in Table 10, the fuels used for power generation in Singapore can be classified into five categories. These fuels are denominated in different units in their respective markets as seen in Table 11.

Because of these different denominations, a conversion factor is necessary in Eq. (5). Except for energy-denominated natural gas, petroleum fuels and coal might have different values depending on the source and the particular petroleum product / blend.

Table 11 Fuels for power generation including their denomination and conversion factors

Fuel	Denomination	Conversion Factor
PNG	$mmBTU$ (energy)	$3.412\ \frac{mmBTU}{MWh}$
LNG	$mmBTU$ (energy)	$3.412\ \frac{mmBTU}{MWh}$
Petroleum products	$oil\ barrel$ (volume)	$0.578\ \frac{bbl}{MWh}$ [7]
Coal	$metric\ ton$ (mass)	$0.143\ \frac{ton}{MWh}$ [8]
Incinerable wastes	*not applicable;* as it is not purchased by Waste-to-Energy plants	-

b) Thermal efficiencies and part-loading

Thermal power plants can be characterized by their thermal efficiencies and their part-load performance (i.e., how their efficiencies drop from full-load to partial loading). As discussed in Section 2.6, the full load efficiencies of the power plants had to be selected from the typical range of values listed in Table 14. Furthermore, to model uncertainty and variability upon operation, a skewed normal random variable was used. This allowed up to about 5% reduction in efficiency determined the full load efficiency in *every* market period.

This random variable was implemented with the *SciPy* statistics module represented in Eq. (7), and seeded as listed in Annex A.

$$stats.skewnorm(a = -10, loc = \eta_{e_{FL}}, scale = 0.02) \qquad (7)$$

where $\eta_{e_{FL}}$ is the nominal full load efficiency. Such a random variable is shown in Figure 5.

The part-load performance is modelled in Eq. (5) by an output-dependent η_e, and it is portrayed as efficiency curves as in Figure 6. This figure shows the obtained efficiency curves of CCGT and steam turbine plants, which were randomly assigned to all the generating units. Modeling the part-load characteristic of power plants is the basis for calculating the marginal costs at various output levels, which is necessary to calculate bids at marginal cost.

[7] Based on Dubai crude.
[8] Based on Australian coal.

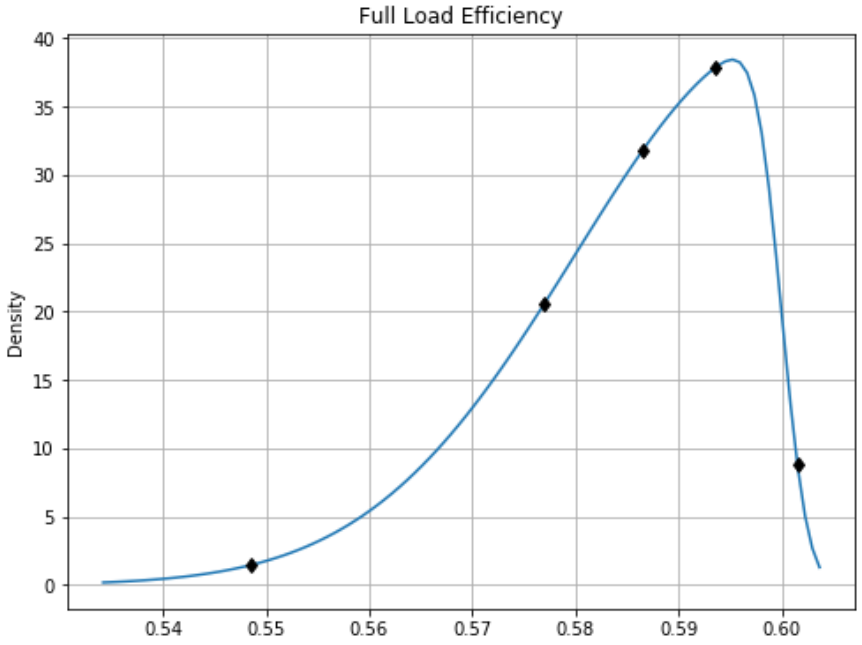

quartiles, 1st and 99th percentiles marked

Figure 5 Full load efficiency skewed normal density distribution

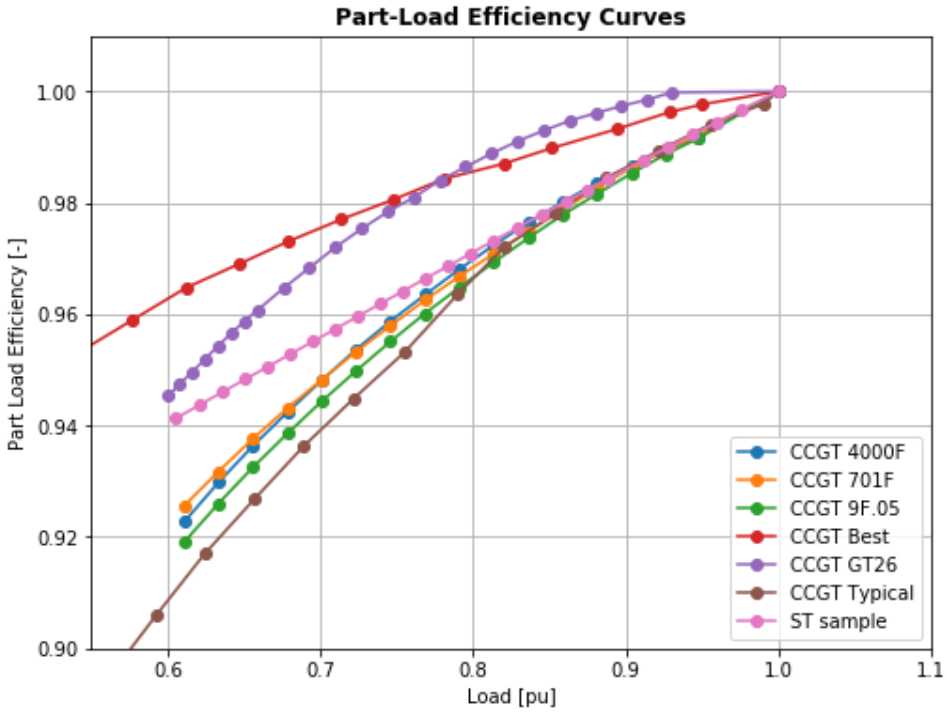

Figure 6 CCGT and steam turbine efficiency curves

Adapted from (PA Consulting Group, 2018) (Strbac & Aunedi, 2016) (Karakurt, 2017)

Bidding behavior

In the NEMS model, the generator companies must submit half-hourly bids of up to 10 $(P_o, \frac{S\$}{MWh})$ quantities. To standardize the bidding, the full allowed output levels of the generators were taken evenly in ten steps, from P_{min} to P_{max}. The discrete $SRMC$ given in Eq. (6) was computed across these steps. A sample calculation is shown in Figure 7.

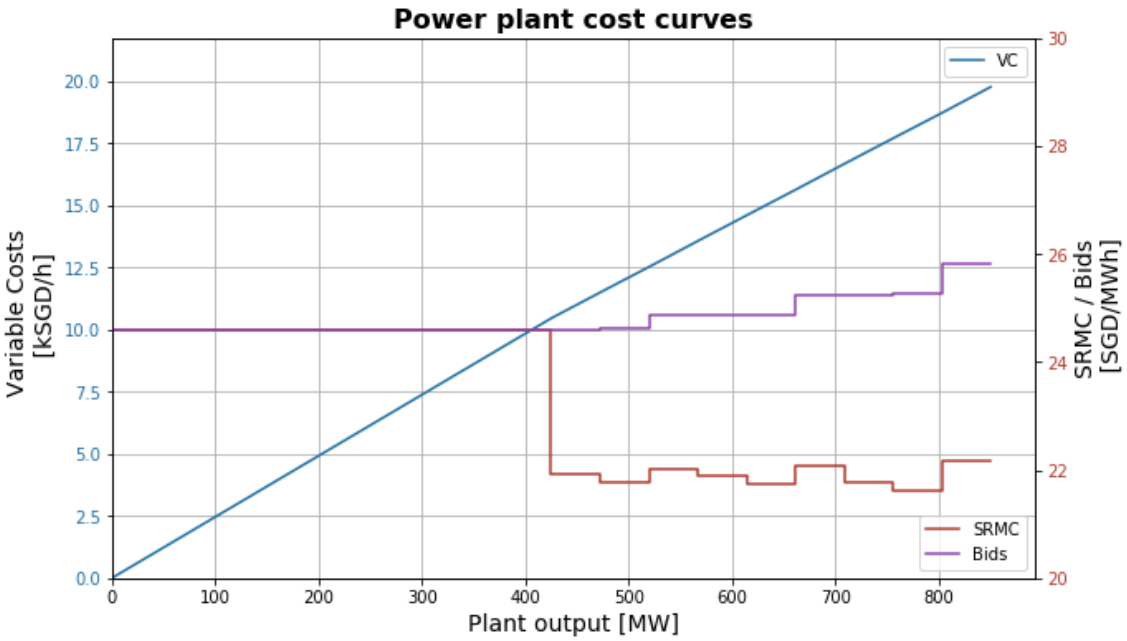

Prime mover	CCGT
Output limits	425 MW - 850 MW
Fuel	PNG (HH)
Fuel price*	3.217 S$/mmBTU
Full load efficiency*	47.24%
Efficiency curve	CCGT Best

**For this calculation only*

Figure 7 Sample cost curves and resulting bids for Senoko CCP 1 and 2

As can be seen in Figure 7, the marginal costs $SRMC$ given in Eq. (6) can lead to non-monotonic curves. However, bids must be increasing monotonically to make the optimization convex. Thus, the calculated $SRMC$ was post-processed according to the simple rule described in Algorithm 2, where succeeding bids are shifted if there is no increase in price of the next bid. This procedure leads to monotonic bids that preserve the original increasing steps in $SRMC$.

Algorithm 2 Process discrete $SRMC$ to a monotonously increasing function

for bid_i *in* $(bid_0, bid_1 \dots bid_9)$*:*

if bid_0*, skip*

if $Price_{i-1} \geq Price_i$*,*

$Price\ Shift = Price_{i-1} - Price_i + 0.10\ S\$/MWh$

Shift the price of all bids from bid_i *to* bid_9 *by* $Price\ Shift$

2. Bidding of fossil-based cogeneration plants

The procedure for calculating the bids of cogeneration plants is identical to that of power-only plants, until the application of Algorithm 2 to the raw $SRMC$. The only difference is in valuing the cogeneration heat. As marginal cost bidding is all about determining the *minimum* price per output level, cogeneration plants can accept a *lower* price for their electricity, if they are certain that they could compensate this via their revenues from heat.

Thus, the bid prices processed by Algorithm 2 can be reduced by the value of heat in Eq. (8), wherein the heat is valued according to the avoided cost of producing the heat directly with a fictitious boiler using the same fuel (Ferreira, Nunes, Martins, & Teixeira, 2014).

$$value\ of\ cogen\ heat\ [\frac{S\$}{MWh_e}] = HPR\ \cdot \frac{1}{\eta_{boiler}} \cdot conversion_{\ fuel}\ \cdot\ Price_{fuel} \tag{8}$$

In Eq. (8), HPR is a parameter derived from the efficiencies of the cogeneration plant, and is assumed to be fixed, as given by:

$$\eta_{total} = \eta_e + \eta_q \tag{9}$$

$$HPR = \frac{\eta_q}{\eta_e} \tag{10}$$

Because the heat market and respective supply contracts are beyond the scope of this model, we imposed no heat supply and demand constraints on the model. Figure 8 shows a sample of a cogeneration station's cost and bid calculation.

3. Bidding of Waste-to-Energy plants

Waste-to-Energy (WtE) plants have a different cost structure, and instead derive revenue from their fuel (National Environment Agency, 2020). We limited our scope to estimating

generation costs based on fuel, and thus we modelled WtE plants to bid at a pre-defined P_o schedule at nearly 0 S$/MWh[9]. This schedule was derived from the 'Others' fuel category in the monthly fuel mix output dataset Table 7. The average MW output of all WtE plants was calculated from these monthly totals, *assuming* that they were online 100% of the time and then allocated via MW capacity. This schedule is shown in Table 12. However, as described in the calibration procedure in Section 3.1, this schedule can be scaled slightly until plant capacities are reached.

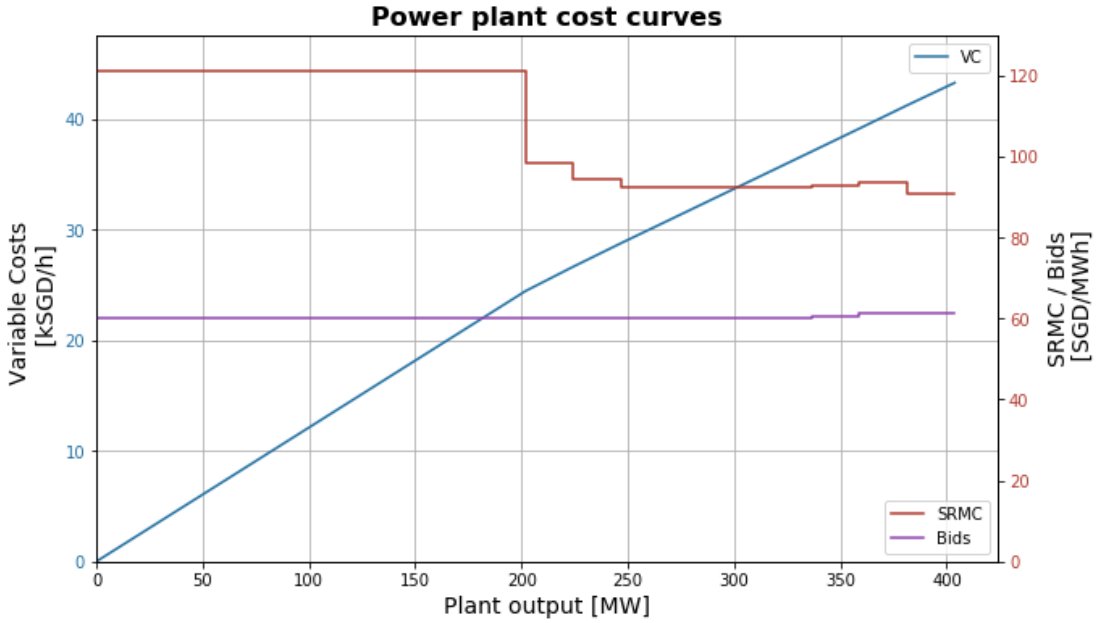

Prime mover	Cogen CCGT
Output limits	201.9 MW - 403.8 MW
Fuel	LNG (JKM)
Fuel price*	11.86 S$/mmBTU
Full load electrical efficiency*	34.18%
Power and heat efficiency	83.00%
Efficiency curve	CCGT 9F.05

**For this calculation only*

Figure 8 Sample cost curves and resulting bids for Sembcorp Cogen @ Banyan

[9] Because the resulting clearing prices were always positive, this bids were always accepted.

Table 12 Waste-to-Energy plant output MW schedule

Month	Tuas Incineration Plant	Tuas South Incineration Plant	Senoko Waste-to-Energy	Keppel Seghers Tuas Waste-to-Energy Plant
Jan	42.3	70.5	48.5	19.4
Feb	44.0	73.4	50.5	20.2
Mar	40.7	67.9	46.7	18.7
Apr	39.2	65.3	44.9	18.0
May	40.4	67.4	46.3	18.5
Jun	38.8	64.7	44.5	17.8
Jul	37.10	61.83	42.51	17.00
Aug	36.63	61.06	41.98	16.79
Sep	46.64	77.73	53.44	21.38
Oct	40.52	67.53	46.43	18.57
Nov	37.25	62.08	42.68	17.07
Dec	41.14	68.56	47.14	18.85

b) Outages

Power plants outages were modelled in the system based on the theory of repairable systems (Cassady & Pohl, 2003) (NIST/SEMATECH, 2013). A homogeneous Poisson process was chosen, being the simplest repairable system model defined by:

1. binary online/offline state, with starting state S_0
2. Intervals i) time to fail T and ii) repair time D are independent and identically distributed exponential variables, parametrized by failure rate λ and repair rate μ, respectively[10]. Eqs. (11)-(12) define these, with t representing the time since the last state change.

$$T(t) = \lambda e^{-\lambda t} \tag{11}$$

$$D(t) = \mu e^{-\mu t} \tag{12}$$

[10] This random failure mode occurs at the flat-portion of the Bathtub Curve (NIST/SEMATECH, 2013), which represents the system life between early failure and failure due to age. This was assumed for all plants, regardless of asset age.

Having a single failure mode, these outages represented both planned and unplanned outages. This resulted in a set of online generators for every market period, and only the online units participated in the bidding process.

There are four related metrics that characterize the reliability of repairable systems given by Eqs. (13)-(14).

$$A_{lim} = \frac{MTTF}{MTTF + MTTR} \tag{13}$$

$$AF = \frac{1}{MTTF + MTTR} \tag{14}$$

where,

A_{lim}	Limiting availability; the probability that the system is available at any given time
AF	Average failures (expressed per year in the power plant database, but in the same units of time in (14))
$MTTF$	Mean Time to Fail
$MTTR$	Meant Time to Repair

These metrics are more descriptive than the parameters of the exponential variables (λ and μ), which for a homogeneous Poisson process are given by Eqs. (15)-(16). Note that the specification of any two independent quantities of these six would fully specify the availability of the generation units. Section 3.c describes how these parameters were set.

$$\lambda = \frac{1}{MTTF} \tag{15}$$

$$\mu = \frac{1}{MTTR} \tag{16}$$

Once parameters λ and μ have been determined, the online status of all generating units is determined prior to the market process. Each generating unit may start online or offline, described by a binary variable with probability $P(1) = A_{lim}$ which is sampled at the beginning of the simulation. The three random variables T, D and S_0 were seeded as listed in Annex A, and the results of this outage simulation are summarized in Figure 13.

c) Internal energy flows and waste heat streams

To pass the waste heat emissions of power plants into WRF, they have to be disaggregated into a) sensible heat into the atmosphere, b) latent heat into the atmosphere, and c) heat into the sea. Let these be referred to as heat streams *by kind*. This was done by:

1. Calculating the *full load* internal energy flows per generator unit as in Figure 1 and resolving the waste heat released via the stack, condenser and other losses (includes auxiliary plant loads and miscellaneous losses). Collectively, these are referred to as heat stream *by outlet*. These are specified in per unit of the input fuel HHV.

   Some of the assumptions made in this step include:
   i. The steam turbine-to-gas turbine output ratio in CCGT plants is 1:2.
   ii. Cogen CCGT plants use a back-pressure ST, and thus have no condenser.
   iii. Typical ST efficiencies ranging from 35%-47% were used.

2. Scaling of the heat stream by outlet percentages according to the simulated electrical full load efficiencies (factoring the fixed HPR for cogeneration), per market period. Let this be k, and is given by Eqs. (17)-(18).

$$k_{power\text{-}only} = 1 - \eta_e \tag{17}$$

$$k_{cogen} = 1 - \eta_e(1 + HPR) \tag{18}$$

3. Resolving the adjusted heat streams by outlet into heat streams by kind according to the following rules:

   a. stack heat

      Contains the latent heat of combustion expressed in per unit fuel HHV as

$$stack\ latent\ heat, per\text{-}unit = \frac{HHV_{fuel} - LHV_{fuel}}{HHV_{fuel}} \tag{19}$$

      with the remainder of the stack heat set as sensible heat into the air.

   b. condenser heat

      Depending on the condenser cooling system described in Table 5, the condenser heat was set as 100% sensible for dry cooling systems, and 100% heat into seawater for once-through systems.

c. other heat losses – assumed to be 100% sensible heat into the air

2.6 Baseline Calibration

Due to some missing parameters to specify the model, we had to calibrate the model under the baseline defined by the system demand and fuel prices in 2016 to be as consistent as possible to the monthly generation and fuel consumption data described in Section 2.3.

a) Loss function

The model was calibrated via hyperparameter optimization based on Bayesian optimization (Bergstra, Yamins, & Cox, 2013). The calibration uses the Tree of Parzen Estimators search algorithm[11], and was solved over a full year of 2016. The loss function of the model was expressed in units of ktoe as:

$$Loss = w_{out\text{-}mix} \sum_{fuel} \omega_{fuel} RMSE_{out\text{-}mix}^{fuel} + w_{in\text{-}mix} RMSE_{in\text{-}mix} + w_{LNG} Loss_{LNG} + w_{cogen} Loss_{cogen} \quad (20)$$

where,

$w,\ \omega$	weights, with $\sum w = 1, \sum \omega = 1$
$RMSE_{out\text{-}mix}^{fuel}$	RMSE of the fuel mix, per fuel in {natural gas, petroleum products, coal, others[12]}
$RMSE_{in\text{-}mix}$	RMSE of the input fuel mix
$Loss_{LNG}$	LNG loss component
$Loss_{cogen}$	Cogen loss component

The selection of weights is shown in Table 13. The fuel mix by output component was prioritized, as this best represented the distribution of the load amongst power plants. Next was the fuel mix by input, which describes the total energy input to power generation and thus the total unconverted heat.

[11] As implemented in *hyperopt*: https://hyperopt.github.io/hyperopt/

[12] In this model, the "Others" fuel category was equated to waste, because the other sources contributed trace amounts to the fuel mix.

The RMSE of the output component was specified on a per-fuel basis to allow more weight to the smaller contributions of petroleum products and coal, in an effort to reduce the relative errors.

Table 13 Choice of weights in the error expression

Error components	$w_{out\text{-}mix} = 0.53$, $w_{in\text{-}mix} = 0.26$, $w_{LNG} = 0.13$, $w_{cogen} = 0.08$
Output-mix fuel weighting	$\omega_{NG} = 0.05$, $\omega_{PP} = 0.45$, $\omega_{Coal} = 0.45$, $\omega_{Others} = 0.05$

In Eq. (20), two loss components for LNG consumption and the cogeneration heat were introduced as piecewise linear penalties:

$$Loss_{LNG} = \begin{cases} 0.9\, Import_{LNG} - E_{LNG}, & 0.9\, E_{LNG} < Import_{LNG} \\ 0, & otherwise \end{cases} \quad (21)$$

[13]

$$Loss_{Cogen} = \begin{cases} Q_{cogen} - Q_{cogen\ ub}, & Q_{cogen} > Q_{cogen\ ub} \\ 0, & otherwise \end{cases} \quad (22)$$

where,

E_{LNG}	LNG consumed for power generation, in ktoe
$Import_{LNG}$	LNG imports, in ktoe
$Q_{cogen\ ub}$	Estimated upper bound on the total cogeneration heat from (Kayanan, Resende Santos, Ivanchev, Fonseca, & Norford, 2019)

[13] Solutions with E_{LNG} larger than the total imported LNG were rejected.

b) Calibration Parameters

The valid ranges for the calibration parameters are summarized in Table 14. The electrical efficiency parameters were based on (US Energy Information Administration, 2019), (IPIECA, 2014) , (Wärtsilä, 2020), (Guinness World Records, 2018), and (National Environment Agency, 2020).

The average power plant failures per year was set to a max of two outages per month, and the lower bound for the limiting availability was estimated as described in the previous section. The other bounds of both parameters are limiting cases and were simply estimated.

Table 14 Calibration parameter ranges

Parameter	Range	
Full load electrical efficiency [%]	CCGT	45%-63%
	OCGT	33%-44%
	Cogen CCGT	34%-40%
	Cogen ST	22%-40%
	ST	30%-42%
	WtE	17%-24%
Average power plant failures [yr^{-1}]	1 - 24	
Limiting availability [-]	0.80 - 0.97	

2.7 Scenario simulation and calculation of waste heat streams

As discussed in Section 1.2, the problem was divided into first calculating the power plant dispatch ($P_o(t)$ for every unit and $Q_{cogen}(t)$, if applicable), and then resolving the waste heat per power plant into heat streams for WRF. We achieved the first step by calibrating the model to the 2016 baseline scenario and re-running the model for new scenarios over the full year, such as the full electrification of road transportation discussed in Section 3.4.

We then proceed with the second step by taking the month of April for further processing of the waste heat as described in Section 2.5c). The inputs were specified as shown in Table 15.

Table 15 WRF input specifications

Specification	Description
Temporal	• 30 days of April 2016 • hourly resolution, obtained by taking the average of 30-min periods
Spatial	• waste heat streams per WRF grid cell (300 m-by-300 m)
Heat streams	• sensible heat into the air • latent heat into the air • heat into the sea
Units of heat streams	• W/m^2; as the stack and condenser cooling systems fit well inside a WRF grid cell, the heat values were divided by the cell area
Emission height	• Sensible and latent heat emissions assumed to be released at the stack height. • Heat into the sea set at sea level

3 Results and Analysis

3.1 Baseline calibration and model accuracy

The calibration of the baseline was performed over 415 trials[14]. Trial 208 yielded the best results, with a loss decline of 31.8% of the mean loss of the first ten trials. The best parameters can be found in Annex A, Table A2. The model downscaled a total waste and cogeneration heat of **5195 ktoe**, which is within **1.88%** of our estimate based on energy statistics. The accuracy is judged on two levels: 1) the dispatch, or where the electricity is sourced; and 2) the fuel consumption and thereby heat released by the power plants.

a) Dispatch accuracy

Figure 9 shows the monthly electricity produced per major fuel, comparing the model and the statistics. The errors, which cancel out due to electricity balance, are summarized in Figure 10. We observe that the model was able to replicate most of the electricity production coming from natural gas, and more accurately so compared to other fuels. As this group comprises four power plant classes representing over 10,300 MW of the 13,445 MW fleet, this suggests

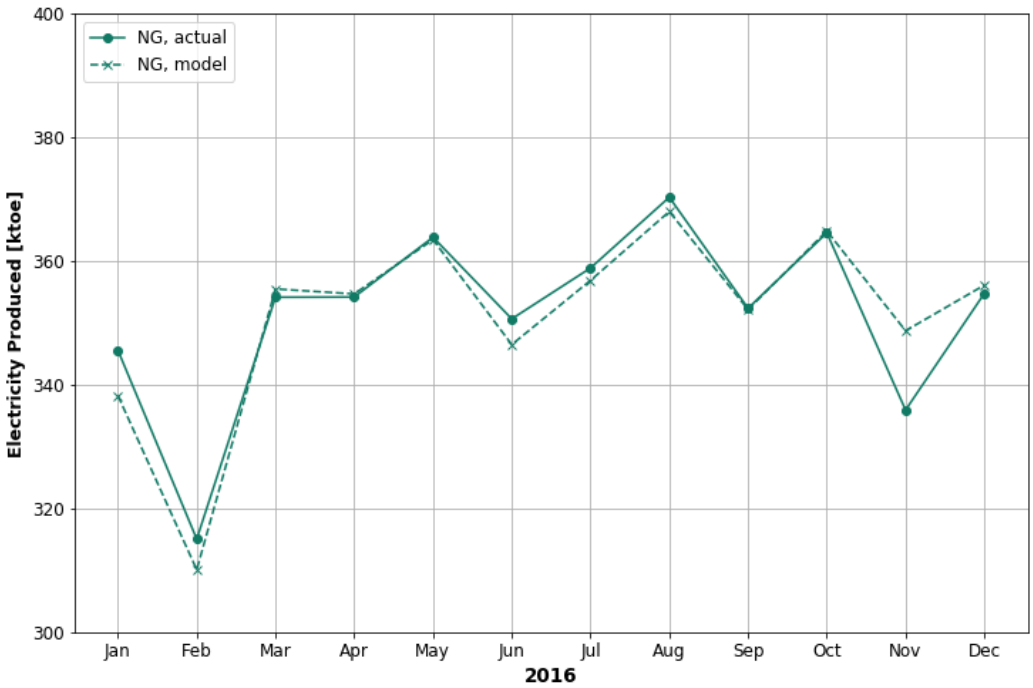

a) natural gas

[14] A trial worth one year of simulation time typically takes 120 s -130 s on a laptop with an Intel® Core™ i5-5200U processor and 8 GB of RAM.

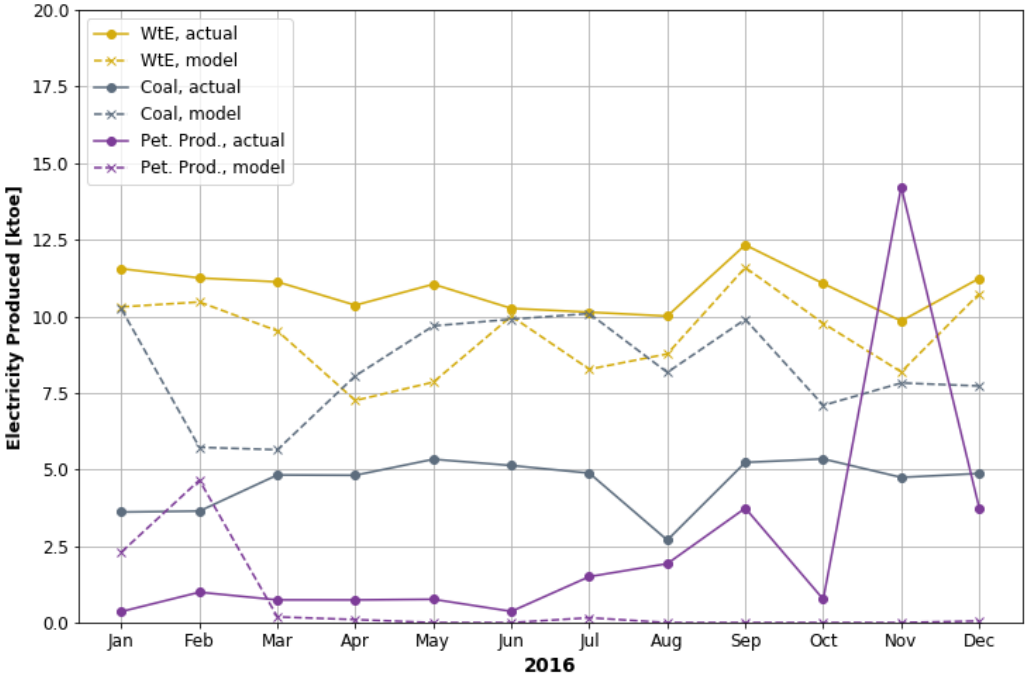

b) all other fuels

Figure 9 Monthly electricity produced per major fuel, model vs. actual

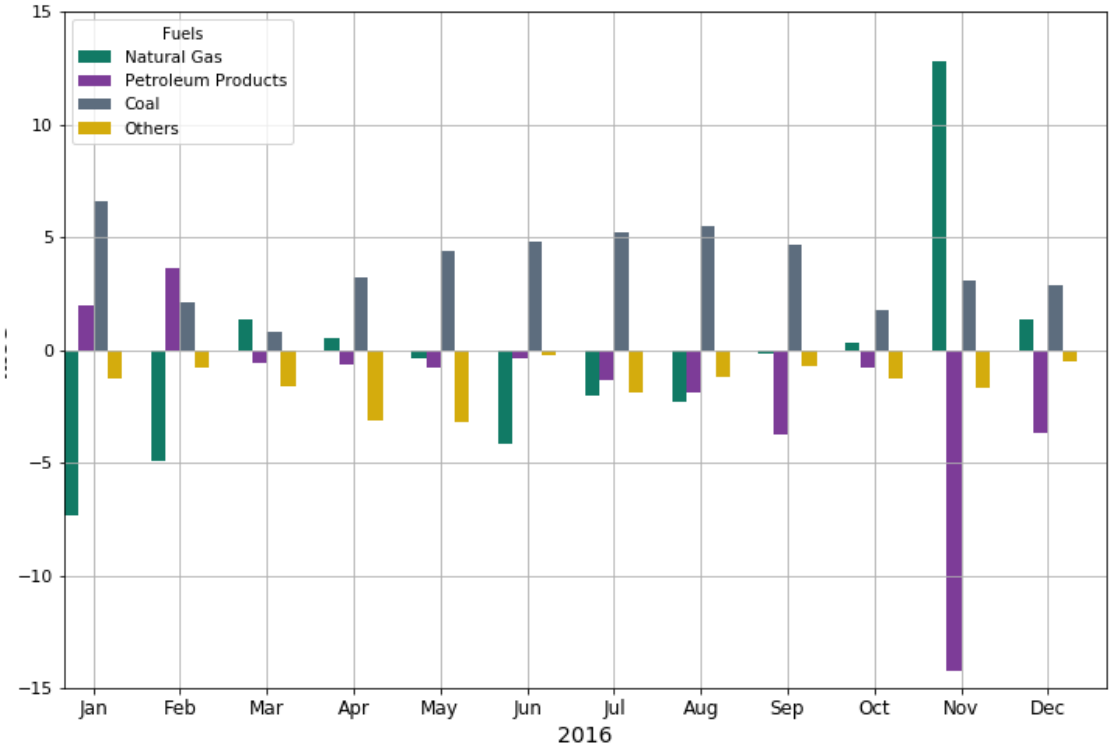

Figure 10 Fuel mix errors of monthly electricity produced per major fuel

Note: Monthly error terms sum to zero due to electricity balance.

that the high degree of freedom made the calibration of these plants effective. However, the allocation amongst natural gas plants is unknown, and the model can only infer this by relying on the economics of power generation. This is further discussed in the *Summary* section.

On the other hand, the coal power plants are generally overestimated and oil plants are mostly underestimated; this suggests that coal was comparatively cheaper in the model than it was in reality, and vice-versa for oil. By considering the relative movement of fuel prices plotted in Figure 11, we can see that oil prices went on an upward trend from the start of the year. In this regard, relying on the proxy fuel prices does *not* explain the dispatch of coal- and oil-fired plants and we need to get more reliable price data, as well as potential supply limitations in the case of coal.

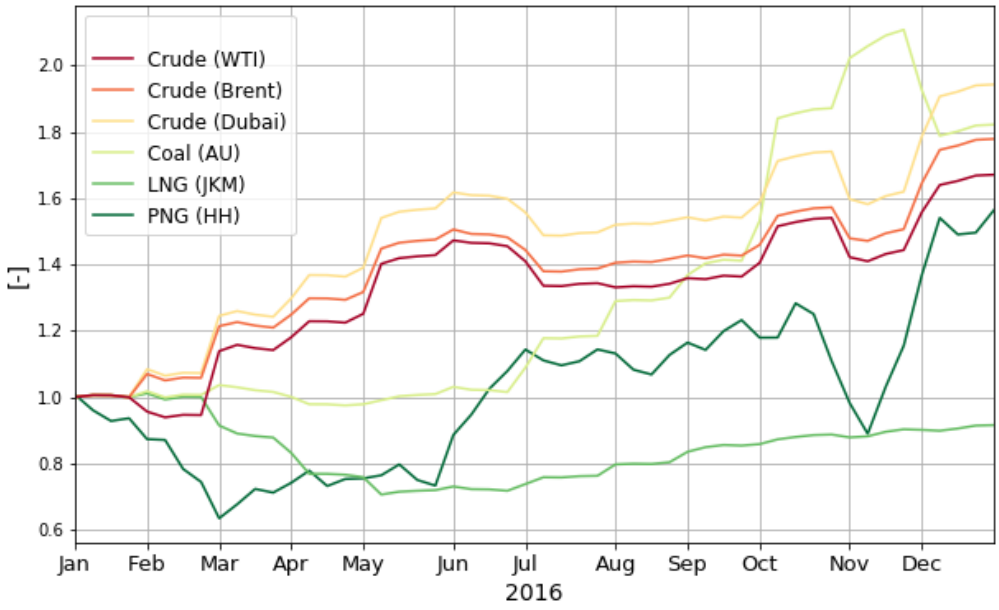

Figure 11 Relative fuel price movement

Finally, waste-to-energy (WtE) plants are generally underestimated. This is expected, because the WtE schedule was computed as if the plants experienced no downtimes (see Section 2.5)[15]. The RMSE of the monthly electricity production along with the annual fuel consumption are summarized in Table 16.

b) Fuel and heat accuracy

Table 16 relates the accuracy of the electricity production and fuel consumption per major fuel. The annual fuel consumption errors are inherently larger in magnitude primarily because of the longer period. Despite the good accuracy in the calculated electricity production of

[15] Other calibration attempts that used a parameter to scale the WtE schedule to reduce the error ended up reducing the overall model fit.

natural gas plants, their fuel consumption was overestimated by around 4.5%, leading to more cogeneration and waste heat to this group. On the other hand, you have less heat associated to all other plants, with the outlying case of under-dispatched oil-fired plants. An interesting result in Table 16 is that the errors in the fuel consumption nearly cancel out, leading to the total calculated heat closely matching the Sankey estimate.

Table 16 Accuracy of electricity production and fuel consumption

Fuel	Monthly electricity production		Annual fuel consumption	
	RMSE [ktoe]	Actual Range [ktoe]	Error [ktoe]	Actual [ktoe]
Natural Gas	4.77	315 - 370	374.18	8364.23
Petroleum Products	4.61	0.36 - 14.23	-100.97	122.80
Coal	4.09	2.69 - 5.34	1.66	259.22
Others	1.71	9.85 - 12.33	-179.03	788.60

*Monthly electricity production RMSE weighted by total production of **4.669 ktoe***

c) Summary

Finally, Table 17 summarizes the energy flows per fuel, and compares them to the actual statistics. The computed total heat and cogeneration heat are compared to those based on statistics in Table 18. Most of the electricity and heat releases were allocated accurately to the natural gas fleet, and the other fuels are releasing relatively lower heat but weighs less in absolute terms. Although inexact, the model downscaled the total heat released by power generation in Singapore and described a plausible scenario of heat emissions.

Table 17 Summary of generation energy flows and heat in 2016

Fuel Class	Model			Actual		
	Input Fuel	Output Electricity *[ktoe]*	Waste and Cogen Heat	Input Fuel	Output Electricity *[ktoe]*	Waste and Cogen Heat
Natural Gas	8,738	4,215	**4,523**	8,364	4,220	**4,143**
PNG	6,726	3,492	3,235	-	-	-
LNG	2,012	724	1,288	-	-	-
Petroleum Products	21.83	7.45	**14.38**	122.8	29.86	**92.94**
Coal	260.9	100.1	**160.8**	259.2	55.11	**204.1**
Others	609.6	112.8	**496.8**	788.6	130.2	**658.4**

Table 18 Total power plant heat from model and Sankey estimate

	Sankey Estimate	Model
Total Released Heat	5099 ktoe	5195 ktoe
of which cogeneration heat	2235 ktoe*	1913 ktoe

Total Released Heat within 1.88% of Sankey estimate.

**Estimated upper bound.*

As mentioned in the discussion on dispatch accuracy, there is no data on the actual allocation of electricity within the natural gas plants. The model determined this based on the merit order, and the dispatch statistics are summarized in Table 19. By comparing how closely the capacity factor matches the availability factor, we see that the model dispatched more of the PNG plants being the cheaper fuel, and the cogeneration versions of the CCGT plants, as they provide additional value from process heat. Finally, Table 20 details the resulting loss of the calibration for completeness.

Table 19 Model summary dispatch statistics

Power Plant Class	Availability Factor	Capacity Factor	Average Load [MW]	Total Capacity [MW]	Total Load [ktoe]
CCGT PNG	86%	85%	3,507	4,147	2,649
CCGT LNG	92%	2.5%	51.9	2,057	39.2
Cogen CCGT PNG	89%	89%	1,115	1,255	842.7
Cogen CCGT LNG	88%	33%	906	2,721	684.5
Cogen ST Coal	86%	83%	132	160	100.1
Oil	89%	0.36%	9.9	2,721	7.45
WtE	86%	58%	149	257	112.8

Notes:

Availability Factor = percentage of the online time, over a period of usually 1 year.
Capacity Factor = ratio of the total power plant output over the maximum permitted by the capacity, over a period of usually 1 year.
Capacity Factor ≤ Availability Factor

Table 20 Loss components and overall loss

Loss Component	Weight	Value [ktoe]
$\sum_{fuel} \omega_{fuel} RMSE_{out\text{-}mix}^{fuel}$	0.53	4.248
$RMSE_{in\text{-}mix}$	0.26	213.5
$Loss_{LNG}$	0.13	23.63
$Loss_{cogen}$	0.08	0.000
Overall (weighted)		61.52

3.2 Model behavior and dispatch analysis

In this section, we would demonstrate how well the model results can be linked to basic generation economics as well as the analysis of computed statistics and plots. The generation mix per power plant class is shown in Figure 12, which we would relate to the relative fuel price movements and outages.

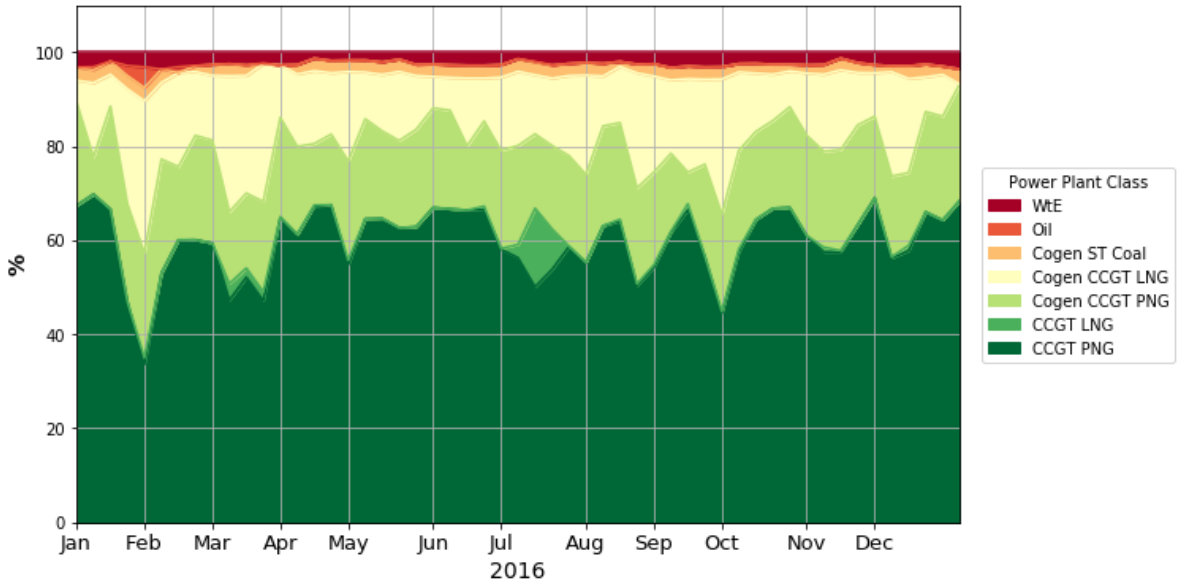

Figure 12 Generation mix by electricity output (baseline)

Natural gas dominates the mix

Figure 12 shows how natural gas dominates the generation mix, and how this is allocated amongst the four natural gas plant classes as summarized in Table 19. Furthermore, we see that the capacity factors of both PNG plant classes approach the availability factors, which means that they are always dispatched and are limited by their outages. However, the PNG CCGT class has a much larger capacity, and thus this class accounted for most of the electricity from natural gas.

Sensitivity of dispatch to outages

The stochastic simulation of outages led to two notable production declines of CCGT PNG plants in Figure 12. The first is a steep descent towards February. The second is a reduction in July accompanied by an uptake in CCGT LNG plants. By referencing these to the online capacities plot in Figure 13, we can confirm that both are due to major outages. Whereas the February outages were compensated by an increase in Cogen CCGT LNG and oil-fired plants, the July outages were compensated by CCGT LNG, as the cheaper Cogen CCGT LNG plants themselves underwent outages. Both incidents were accompanied by relatively cheaper prices of oil in February, and LNG in July (see Figure 11). We can take a closer look at the July dispatch Figure 14.

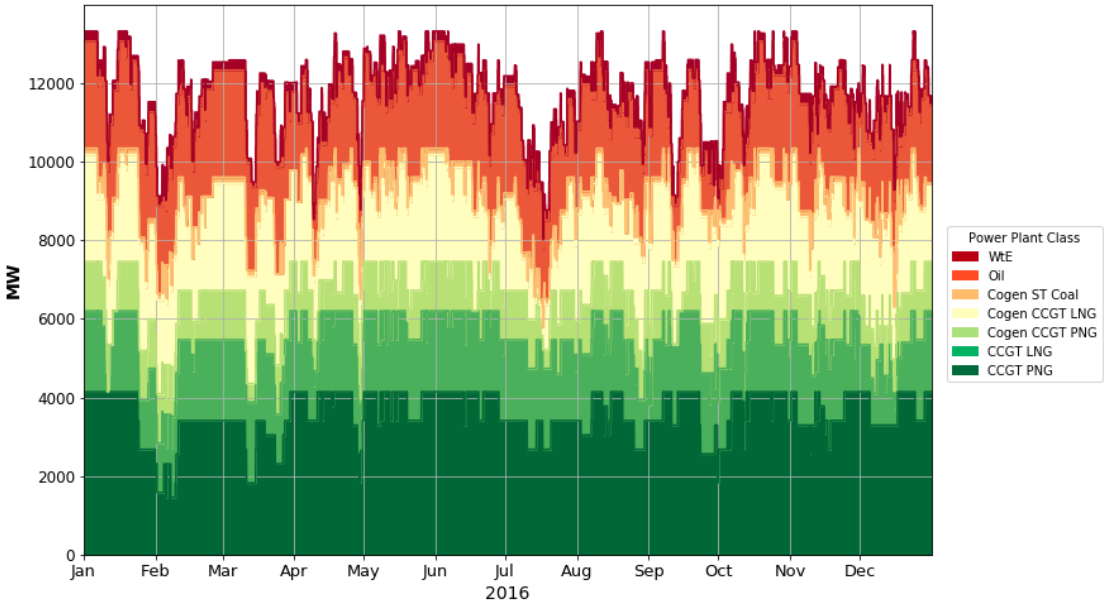

Figure 13 Online capacities (baseline)

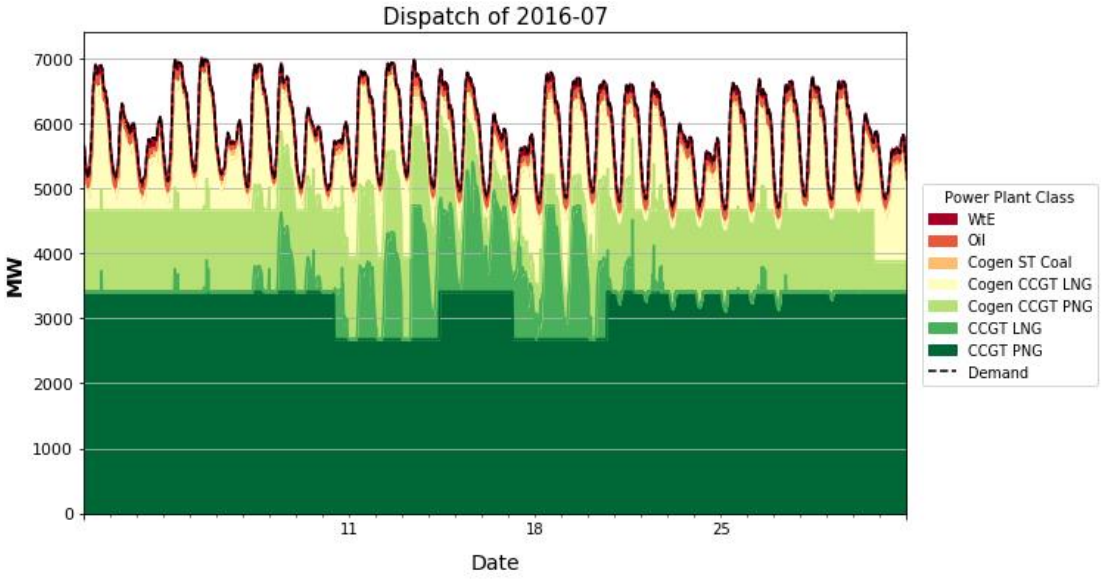

Figure 14 July dispatch (baseline)

LNG plants as the marginal power plants

Figure 14 also shows that the CCGT LNG plants were effectively the marginal plants, as their outputs follow the demand closely. It also suggests that outside these outage events, Cogen CCGT LNG plants act as the marginal plant. We can confirm these by computing the correlation of the dispatch of these power plants with the demand, along with the correlation of CCGT LNG with the demand for this specific period, which can be seen in Table 21. Furthermore, this is supported by the partial capacity factors found in Table 19.

Table 21 Correlation between dispatch and demand

Power Plant Class	Correlation	
	2016	*July 2016, selected*
CCGT PNG	0.23	-
CCGT LNG	0.17	**0.41**
Cogen CCGT PNG	0.01	-
Cogen CCGT LNG	**0.66**	**0.68**
Cogen ST Coal	0.13	-
Oil	0.10	-
WtE	-0.04	-

Fundamentals – correlation between demand and price

Most research suggests a strong relationship between demand and market prices, although the details of this relationship can be market-specific (Afanasyev, Fedorova, & Popov, 2015). Due to the marginal cost bidding assumption, we then expect the price results of the model[16] to be more tightly correlated with the demand than in reality. We observe this in Table 22, which shows the correlation over annual periods.

Table 22 Correlation between demand and clearing prices

Year	Correlation	
	Actual (USEP)	*Model*
2015	0.278	-
2016	**0.241**	**0.523**
2017	0.295	-

[16] We reiterate that the model is *not* meant to predict electricity market prices.

Fundamentals – cheap oil scenario

To demonstrate how market fundamentals drive the model outcomes, we simulated a cheap oil scenario, wherein Dubai crude was down 50% of its original level. The generation mix is plotted in Figure 15. Oil-fired plants clearly displaced Cogen CCGT LNG plants, which were identified as the marginal plants in the base scenario.

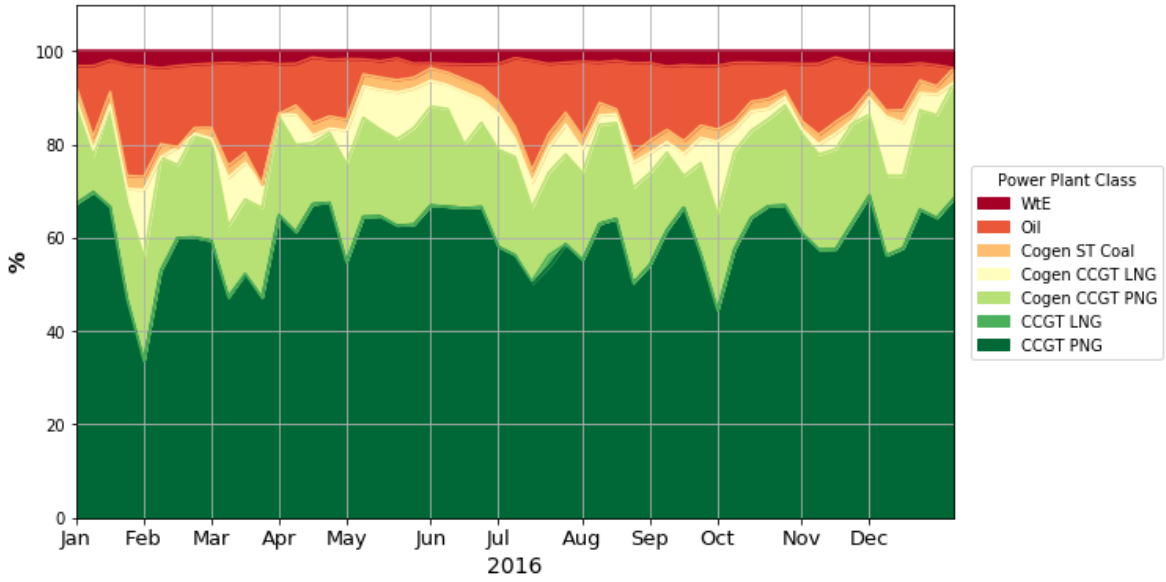

Figure 15 Generation mix by output electricity in cheap Dubai crude scenario
Oil-fired plants capacity factor=24.9% (up from 0.36%)

3.3 Heat analysis

In this section, we will analyze how the dispatch results discussed in the previous section translate to the heat produced by power plants. Figure 16 plots the energy distribution in the fleet, in terms of their electricity production and associated heat. These values are then summed per power plant class in Table 23.

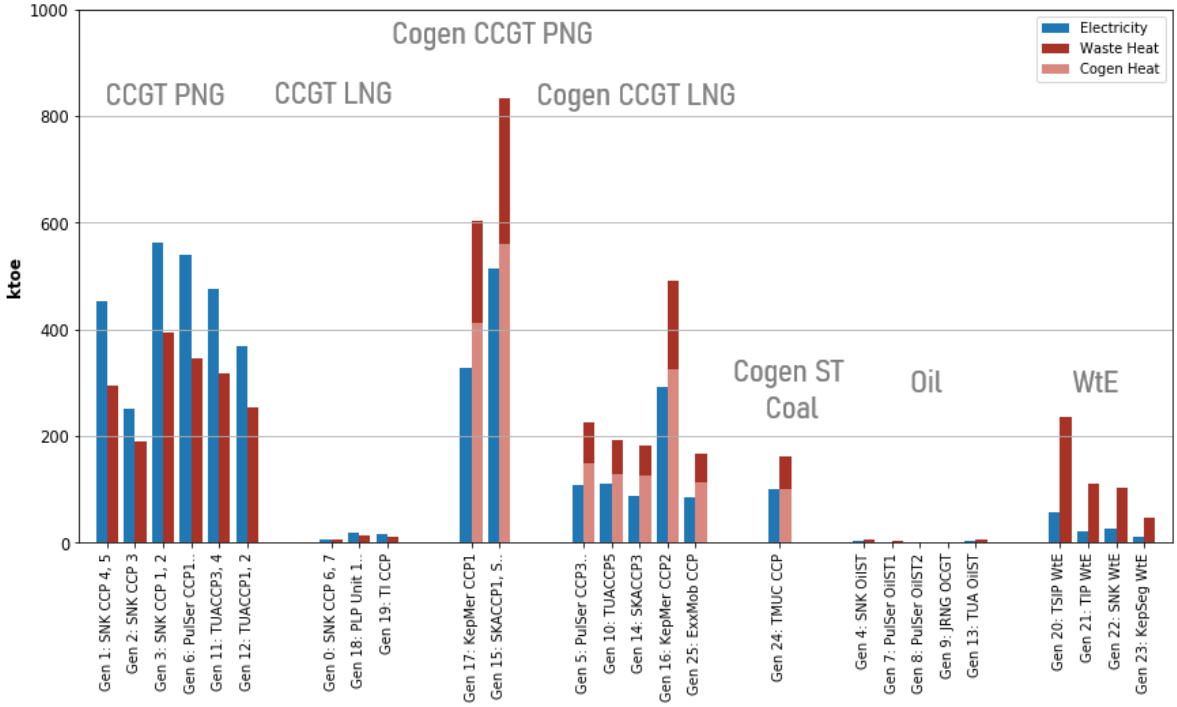

Figure 16 Electricity and heat distribution in 2016 baseline

Table 23 Total heat and cogeneration heat by class

Power Plant Class	**Heat [ktoe]**		
	Total Released Heat	*of which cogeneration heat*	*of which waste heat*
CCGT PNG	1,796	-	1,796
CCGT LNG	31	-	31
Cogen CCGT PNG	1,438	971	467
Cogen CCGT LNG	1,257	842	415
Cogen ST Coal	161	100	61
Oil	14	-	14
Waste-to-Energy	497	-	497
Total	**5,194**	**1,913**	**3,281**

We observe in Figure 16 that cogeneration plants produce more total heat per unit electricity than their non-cogeneration counterparts (i.e., cogeneration plants are operating at lower electrical efficiencies), but the majority of this is cogeneration heat that has economic value. Similarly, waste-to-energy plants also release more heat per unit electricity, but they provide the benefit of waste management by significantly reducing waste volumes.

We further observe that the highly-efficient CCGT PNG plants were responsible for around half of the waste heat emissions, due to their advantageous running costs as well as numbers. In contrast, Cogen CCGT PNG and LNG plants have comparable total heat but less than half waste heat compared to CCGT PNG. A map of the waste heat released by all power plants highlighting the top sources is shown in Figure 17.

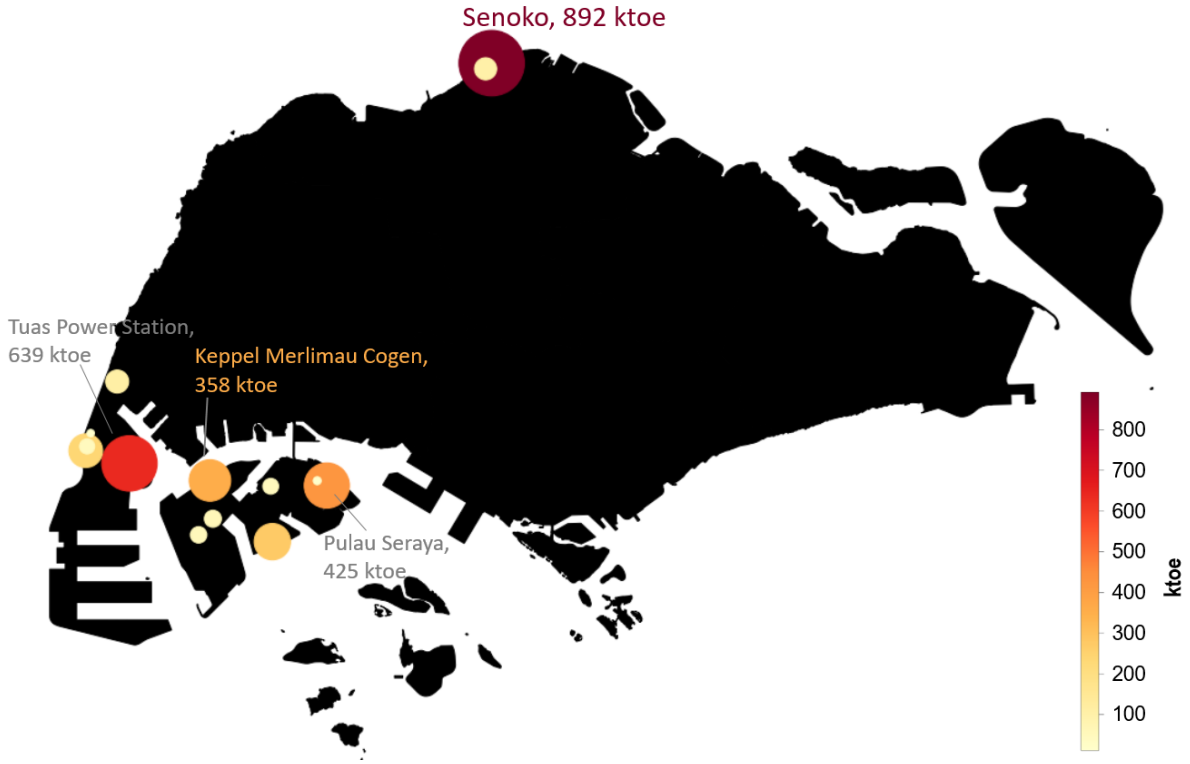

Figure 17 Annual waste heat per power plant in 2016 baseline

Figure 18 shows the waste heat broken down by kind. In the case of the CCGT PNG plants, about half of the waste heat is released into the sea, which comes from their condensers cooled via once-through systems. This is comparable to the CCGT plant in Figure 1, with nearly equal stack heat and condenser heat. Due to the high latent heat of combustion of natural gas given by its HHV/LHV ratio, we can see that the natural gas plants have considerable latent heat. The combined cycle cogeneration plants also show no heat into the sea, following the assumption made that their steam turbines are of the back-pressure type and thus have no condenser. Finally, we observe the highest sensible heat in air released by waste-to-energy plants, because of their dry-cooling systems. A summary is provided in Table 24.

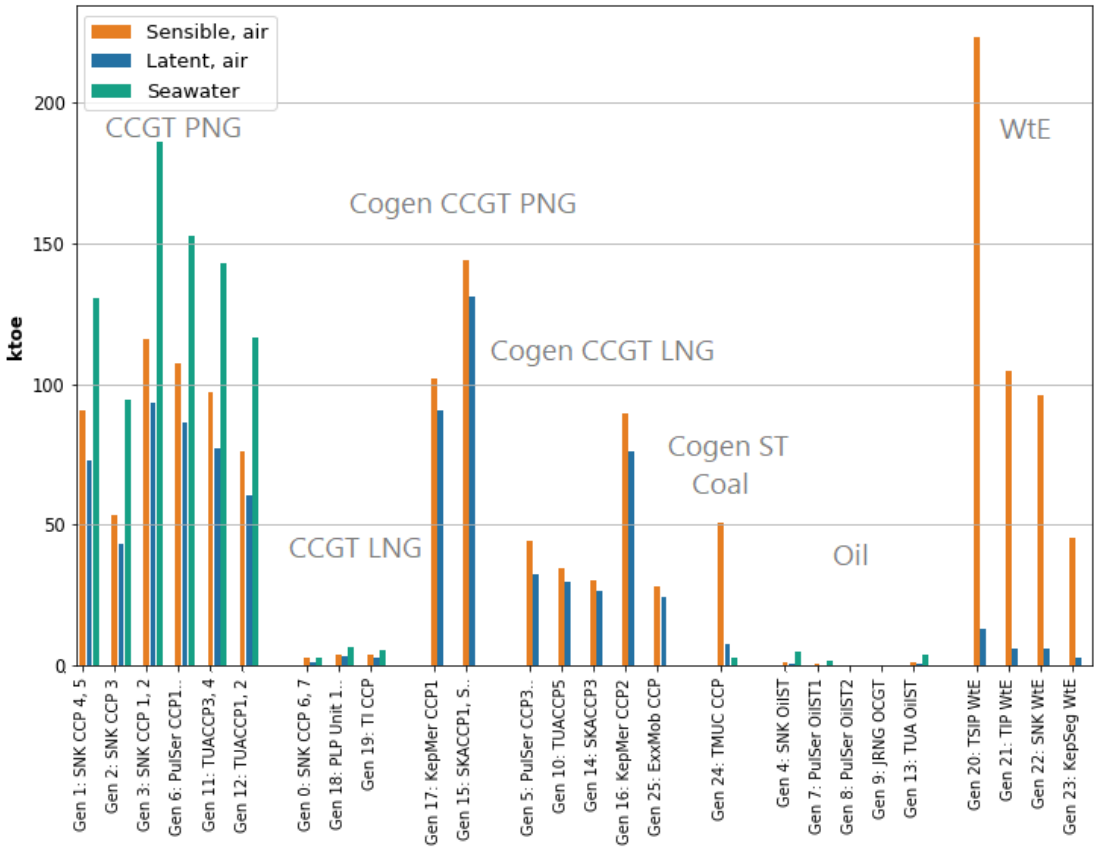

Figure 18 Waste heat streams in 2016 baseline

Table 24 Waste heat streams (ktoe) by generator technology in the 2016 baseline

Waste Heat	CCGT	Cogen *Cogen CCGT and Cogen ST*	ST *Oil-fired and WtE*	Total	
sensible, air	550	523	473	1546	(47%)
latent, air	439	418	28	886	(27%)
seawater	838	2.5	10	850	(26%)

3.4 Full electrification of road transport scenario

The full electrification of Singapore's road transport was modelled and studied as part of UHI mitigation in Cooling Singapore 1.5 (Ivanchev & Fonseca, 2020). A Singapore-wide traffic simulation of a typical day with electric vehicles was done to estimate transport heat emissions and the additional electricity demand for vehicle charging. The latter is shown in Figure 19.

We then simulated the new demand, assuming the profile is repeated over 366 days in 2016. This amounted to a total demand of **369 ktoe**, increasing the peak demand from 7050 MW to 7675 MW and the baseload demand from 4209 MW to 4323 MW.

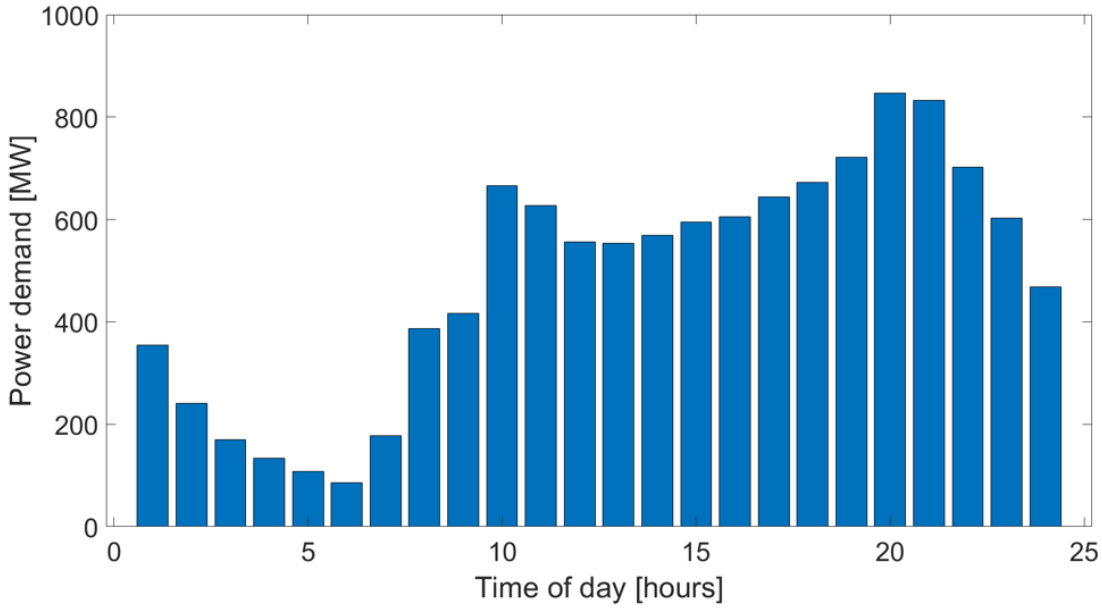

Figure 19 Charging demand in a fully-electrified road transportation system with 20-kW charging stations for Singapore, 2016 (Ivanchev & Fonseca, 2020)

Transportation Fuel Mix

The generation mix is shown in Figure 20, which we can compare with the base mix in Figure 12. We observe that the Cogen CCGT LNG plants have a noticeable increase in the mix, as they were the marginal plant class most of the time in the base scenario. We can then compare this to an average fuel mix, as shown in Figure 21. The more diversified fuel mix in the electromobility scenario is beneficial in terms of energy security, as transportation is no longer fully reliant on oil prices. Furthermore, because of the market-based dispatch, the competition in the power sector makes the transport system more resilient to price shocks to the input fuels.

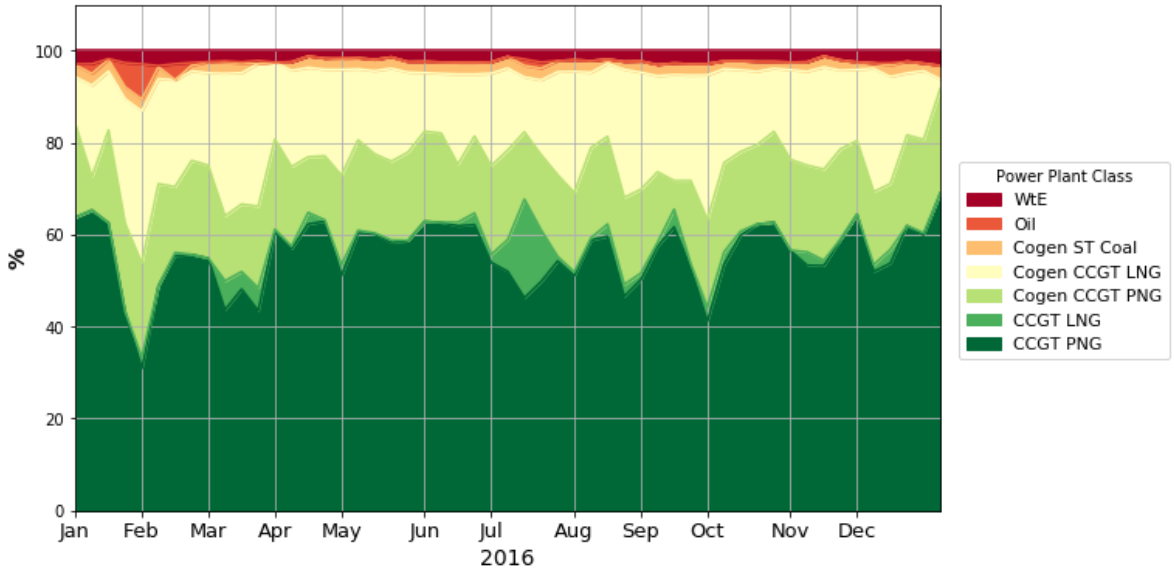

Figure 20 Generation mix by output electricity in full road transport electrification scenario

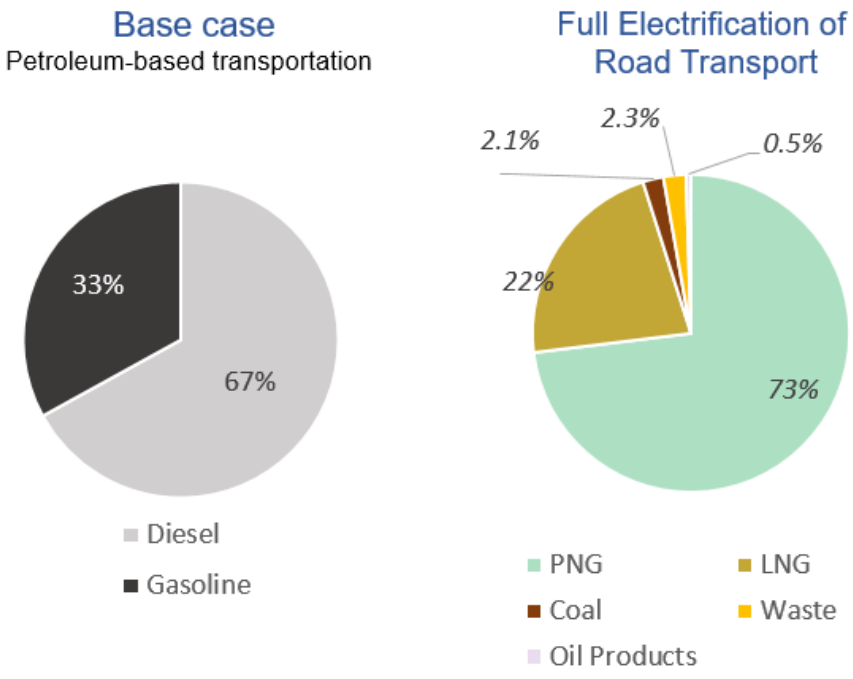

Figure 21 Road transportation fuel mix

Petroleum-based adapted (Ivanchev & Fonseca, 2020)

Baseline petroleum products consumption	*2090 ktoe*
Fully electrified fleet electricity consumption	*369 ktoe*

Added Fuel Consumption

The power sector burned an additional **971 ktoe** of input fuel (890 ktoe of which was LNG) to produce the added **369 ktoe** of EV demand, with an additional cogeneration heat production of **353 ktoe**. The additional fuel consumption is broken down by power plant class in Figure 22, and the total energy flows in the power sector are summarized in Table 25. As discussed in Section 3.2, Cogen CCGT LNG plants were identified as the marginal plants and their capacity factor increased to 47% from a baseline of 33%. Furthermore, this entails an increase in cogeneration heat.

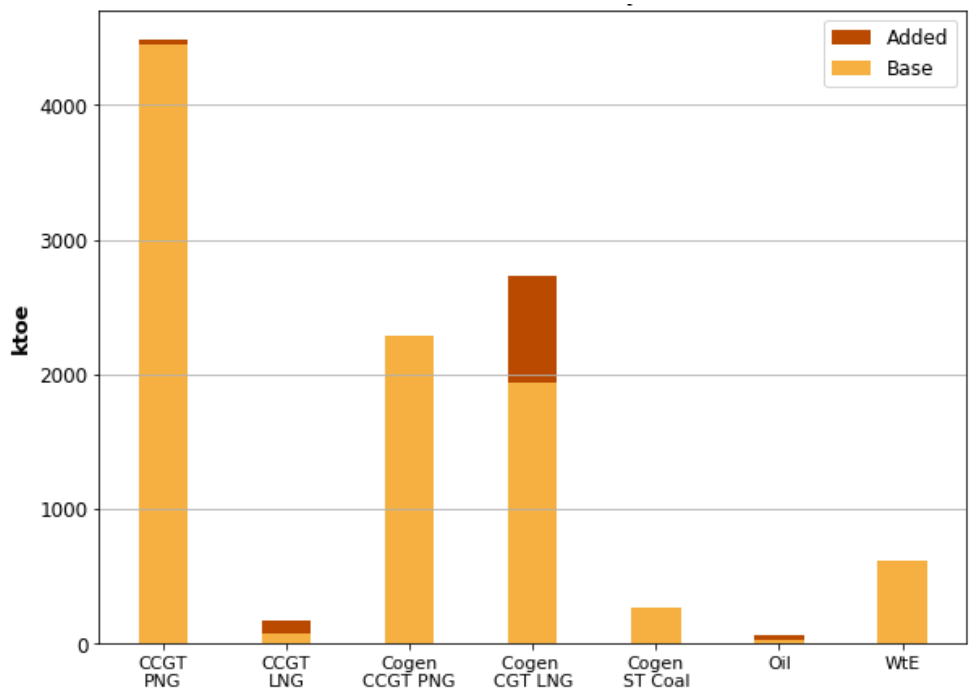

Figure 22 Additional fuel consumption

Table 25 Total energy flows in electricity generation

	Full Road Electrification	Baseline	Delta
		ktoe	
Electricity demand	4,805	4,436	369
Total fuel consumption	10,601	9,631	971
Total heat released	5,796	5,195	601
of which cogeneration	2,266	1,913	353
of which waste	3,531	3,282	248

Anthropogenic heat from power plants and transportation

By switching to a different energy source and using more efficient powertrains, we reduce the heat on the road and shift it to the power plants. We can then compare the heat flux of these two systems. In calculating the heat flux of power plants in kW/m^2, the total waste heat

a) Baseline

b) Electrified transport

Figure 23 Power plant waste heat flux on April 01, 2016 at 7 am

(including sensible, latent and seawater heat) was divided by the WRF grid cell area of 300 m by 300 m. Figure 23 shows the power plant heat maps for the baseline and e-mobility scenario at 7 am, coinciding with the rush hour. We can then compare these to the coincident transportation heat maps in Figure 24. These plots show that whereas you have a dramatic difference in the heat released of petroleum-based and electrified transportation, the shifted heat in the power plants changes relatively little. This is explained both by the small additional power demand of full e-mobility (369 ktoe on top of 4436 ktoe), and the higher combined efficiency of power generation and the electric vehicles. The plots also show that power plant waste heat fluxes can be over two orders of magnitude higher than those of transportation, despite releasing only about 34% more in absolute waste heat in the baseline.

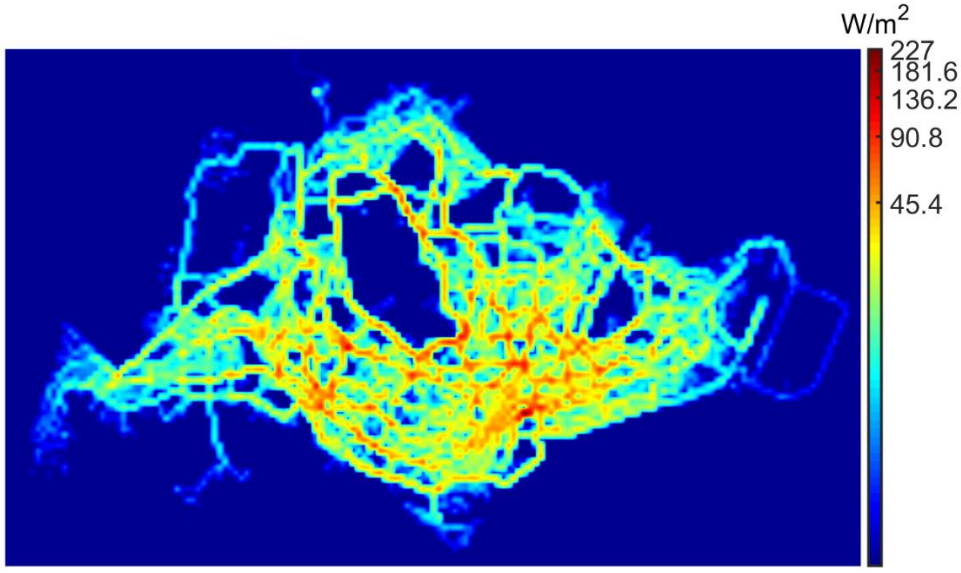

a) Baseline

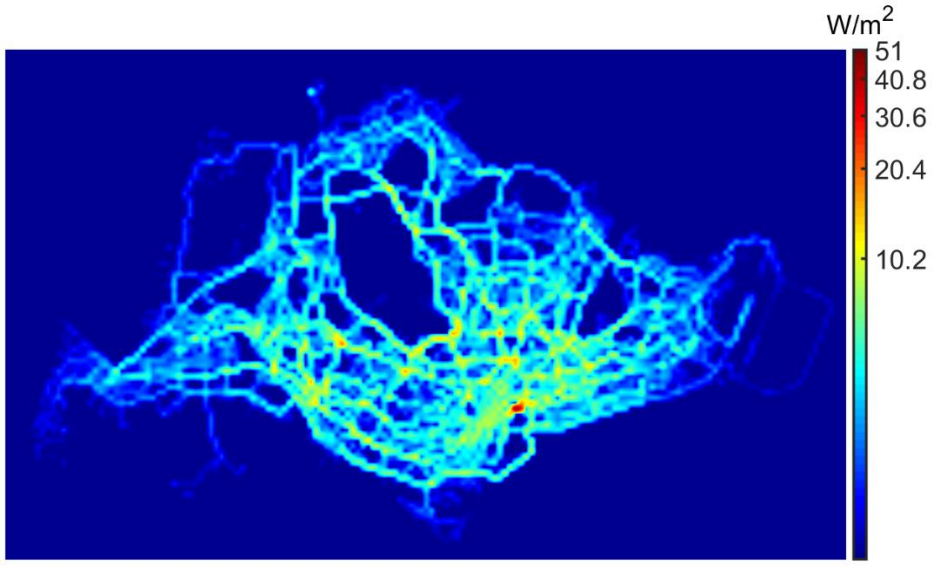

b) Electrified transport

Figure 24 Road transport waste heat flux at 7 am

(Ivanchev & Fonseca, 2020)

Anthropogenic Heat Reduction

Complementing the spatiotemporal perspective, we can compare the change in AH in absolute terms. In our earlier work (Kayanan, Resende Santos, Ivanchev, Fonseca, & Norford, 2019), we accounted the different sources of anthropogenic heat in Singapore and expressed the total AH as the sum of

$$AH_{total} = AH_{Power\ Plants} + AH_{Industry} + AH_{Buildings} + AH_{Transport} + AH_{Misc} \quad (23)$$

where,

$AH_{Power\ Plants}$	The waste heat from power generation (i.e., excluding cogeneration heat)
$AH_{Industry}$, $AH_{Buildings}$, $AH_{Transport}$	The heat from the three energy end-use categories: *Industry*, *Buildings* and *Transportation*. Cogeneration heat has been allocated to *Industry*.
AH_{Misc}	Miscellaneous sources (e.g. human metabolism)

In assessing the AH emissions of this scenario, we make the assumption that *only the anthropogenic heat from transport and power plants would change*. This is important in assessing the change in AH of *Industry*, which can be expressed as

$$AH_{Industry} = Elec + Fuel + Cogen \quad (24)$$

where $Elec$, $Fuel$ and $Cogen$ are the energy demands of *Industry* – electricity, fuels and cogeneration heat. Note that the last two can be combined as the total heat demand. As the power plant dispatch model also outputs cogeneration heat, any changes in cogeneration heat production must be compensated by changes in the *Industry's* fuel demand, so that *Industry's* behavior is unaffected[17]. Therefore, we can calculate the change in total AH as

$$\Delta AH_{total} = \Delta AH_{Power\ Plants} + \Delta AH_{Transport} \quad (25)$$

$$= 248\ ktoe + (369\ ktoe - 2090\ ktoe) = \mathbf{-1473\ ktoe}$$

The modest 248 ktoe increase in waste heat for a 369 ktoe increase in electricity produced is due to the general efficiency advantage of cogeneration (Thorin, Sandberg, & Yan, 2015).

[17] This also ignores any additional efficiencies involved.

Therefore, we can visualize the energy and heat system-effects of full road transport electrification as a change in the anthropogenic heat Sankey diagram in Figure 25, and along the following points:

1. Overall decrease in heat emissions on the roads, from 2090 ktoe to 369 ktoe (**-1721 ktoe or -82.3%**). The electrified Singaporean vehicle fleet is about six times more energy efficient than the petroleum-based one.

2. The additional demand is met mostly by cogeneration plants, leading to a limited increase in waste heat from 3,282 ktoe to 3,531 ktoe (**+248 ktoe or +7.6%**). This heat is ejected in places relatively far away from people and the city.

3. The total anthropogenic heat released in Singapore *decreases* by about -**1473 ktoe**, or about **-7%** of the baseline.

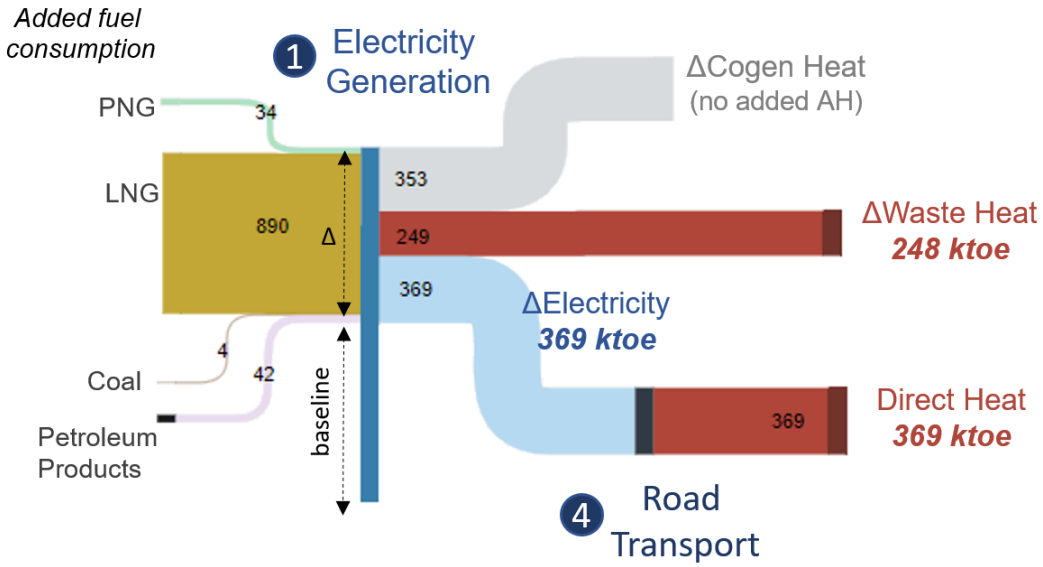

Figure 25 Change in the anthropogenic heat Sankey diagram due to full road transportation

Adapted (Kayanan, Resende Santos, Ivanchev, Fonseca, & Norford, 2019)

4 Conclusions and Recommendations

We modelled the power plant dispatch of Singapore in 2016, based on an energy-only model of its electricity market. Due to the lack of data, we relied on fuel price proxies and calibrated the unknown power plant parameters to match the best available, yet low-resolution official statistics. Nonetheless, the selection of power plants according to merit can still be defined, and we achieved an RMSE of 4.67 ktoe in the allocation of electricity production per fuel and per month. The model accurately allocated production to natural gas plants responsible for 95% of the 4436 ktoe of electricity, but poorly so in the other fuels (e.g. calculated heat from oil plants was only 15% of the actual). Because much of the production was matched, and the calculated total waste and cogeneration heat was within 1.88% of the statistics, we consider this accuracy acceptable for modelling AH at the mesoscale.

The 2016 baseline dispatch is described by fully dispatched PNG combined cycle plants and Cogen CCGT LNG plants as the marginal plants. Accounting for about 30% of Singapore's generation capacity, CCGT PNG plants released over half of the waste heat (1796 ktoe of 3281 ktoe) with the Cogen CCGT-PNG and -LNG plants each releasing comparable total heat, but significantly less waste heat (467 ktoe and 415 ktoe, respectively). We estimate about 1546 ktoe (47%) of the waste heat is released as sensible heat into the air and 886 ktoe (27%) as latent heat, with the rest being dumped into the sea.

We also simulated the response to the full electrification of road transport, wherein the additional 369 ktoe demand came with comparatively little waste heat of 248 ktoe. This is due the additional output of Cogen CCGT LNG plants, being the marginal plants. Overall, this scenario could reduce the total anthropogenic heat in Singapore by 1473 ktoe, or about -7% of the baseline, while shifting the heat from the roads to the power plants.

To improve on our work, we recommend the following courses of action:

1. Use calibration data of a much higher resolution, both temporally and over power plants. With the current development of the model, results are not recommended to be taken at the daily level, but more on a monthly period. If technical power plant data were available, then these data sets can instead serve as validation.

2. Actual fuel prices in Singapore are recommended, including those in long-term contracts and futures. Furthermore, the relatively expensive oil in 2016 might suggest that other power plant operational costs must be considered.

3. Developing other approaches to downscaling the power plant heat, such as statistical models based on dispatch samples, would probably be more useful than implementing more features of the market dispatch. These approaches can then be compared and their results weighted.

References

Afanasyev, D., Fedorova, E., & Popov, V. (2015). Fine structure of the price-demand relationship in the electricity market: Multi-scale correlation analysis. *Energy Economics, 51*, 215-226.

Bergstra, J., Yamins, D., & Cox, D. D. (2013). Making a Science of Model Search: Hyperparameter Optimization in Hundreds of Dimensions for Vision Architectures. *International Conference on Machine Learning.* Atlanta. Retrieved from http://proceedings.mlr.press/v28/bergstra13.pdf

Bhatia, S. (2014, 1 1). Cogeneration. *Advanced Renewable Energy Systems*, 490-508.

Bossel, U. (2003, October 29). *Well-to-Wheel Studies, Heating Values, and the Energy Conservation Principle.* Retrieved from https://www.efcf.com/: https://archives.bape.gouv.qc.ca/sections/mandats/becancour/documents/DC4.pdf

Cassady, C. R., & Pohl, E. A. (2003). Introduction to Repairable Systems Modeling. *Annual Reliability and Maintainability Symposium*(49o).

Chen, Y., Yao, D., Ma, W., Pan, J., Gertmar, L., Babaee, A., & Vesel, R. (2010). Study on coordinated reactive power control strategies for power plant auxiliary system energy efficiency and reliability improvement. *2010 International Conference on Power System Technology* (pp. 1-8). Hangzhou: IEEE.

China Trend Building Press Limited. (2006, June). *Marina Bay, Singapore – Common services tunnel and district cooling system.* Retrieved Dec 2019, from Building.hk: http://www.building.com.hk/forum/2007_0309marinabay.pdf

Coal Marketing International Ltd. (2020). *Coal Basics*. Retrieved from Coal Marketing Info: http://www.coalmarketinginfo.com/coal-basics/

Energy Information Administration. (2007). *Methodology for Allocating Municipal Solid Waste.* Washington DC: U.S. Department of Energy.

Energy Market Authority. (2018). *Singapore Energy Statistics.* Retrieved from Energy Market Authority Website: https://www.ema.gov.sg/cmsmedia/Publications_and_Statistics/Publications/SES18/Publication_Singapore_Energy_Statistics_2018.pdf

Energy Market Authority. (2019, Dec). *Electricity Generated.* Retrieved from Energy Market Authority: https://www.ema.gov.sg/TemStatistic.aspx?pagesid=20140926wbNYp2Yh8iqy&pagemode=live&sta_sid=20140802apItNJRIa9Pa

Energy Market Authority. (2019, Dec). *Generating Plants Availability – Outage & Remaining Capacity.* Retrieved Jan 2020, from Energy Market Authority of Singapore Official Website: https://www.ema.gov.sg/statistic.aspx?sta_sid=20140802QQU3noXxqYwU

Energy Market Company. (2018). *National Electricity Market of Singapore Market Report.* Singapore.

Energy Market Corporation. (2019, Nov). Uniform Singapore Energy Price (USEP) and Demand Forecast (D + 6). Singapore, Singapore. Retrieved Nov 2019, from https://www.emcsg.com/marketdata/priceinformation

Erdem, H. H., Dagdas, A., Sevilgen, S. H., Cetin, B., Akkaya, A. V., Teke, B. S., . . . Atas, S. (2010). Thermodynamic analysis of an existing coal-fired power plant for district heating/cooling application. *Applied Thermal Engineering, 30*(2-3), 181-187.

Feiyu Lu, & Gan, H. (2008). National Electricity Market of Singapore. *2005 International Power Engineering Conference*, 1007-1012 Vol. 2.

Ferreira, A., Nunes, M., Martins, L., & Teixeira, S. (2014). Technical-economic evaluation of a cogeneration unit considering carbon emission savings. *International Journal of Sustainable Energy Planning and Management, 02*, 33-46.

Guinness World Records. (2018, Jan). *Most efficient combined cycle power plant*. Retrieved Jan 2020, from Guinness World Records: https://www.guinnessworldrecords.com/world-records/431420-most-efficient-combined-cycle-power-plant/

International Energy Agency. (2010). *ETSAP Technology Brief 101 - Industrial Combustion Boilers.*

International Finance Corportation. (2008). *Environmental, Health, and Safety Guidelines for Thermal Power Plants.* Washington D.C.: International Finance Corporation.

IPIECA. (2014, Feb). *Open Cycle Gas Turbines*. Retrieved from International Petroleum Industry Environmental Conservation Association official website: http://www.ipieca.org/resources/energy-efficiency-solutions/power-and-heat-generation/open-cycle-gas-turbines/

Ivanchev, J., & Fonseca, J. A. (2020). *Anthropogenic Heat Due to Road Transport: A Mesoscopic Assessment and Mitigation Potential of Electric Vehicles and Autonomous Vehicles in Singapore.* Singapore: Singapore ETH Centre. doi:https://doi.org/10.3929/ethz-b-000401288

JTC. (2020, April 25). *Jurong Island*. Retrieved April 27, 2020, from JTC Corporation website: https://www.jtc.gov.sg/industrial-land-and-space/Pages/jurong-island.aspx

Karakurt, A. S. (2017). Performance analysis of a steam turbine power plant at part load conditions. *Journal of Thermal Engineering, 3*(2), 1121-1128.

Kayanan, D. R., Resende Santos, L. G., Ivanchev, J., Fonseca, J. A., & Norford, L. (2019). *Anthropogenic Heat Sources of Singapore.* doi:10.3929/ethz-b-000363683

Komilis, D., Kissas, K., & Symeonidis, A. (2013). Effect of organic matter and moisture on the calorific value of solid wastes: An update of the Tanner diagram. *Waste Management*, 249-255. doi:10.1016/j.wasman.2013.09.023

Krause, P., Boyle, D. P., & Bäse, F. (2005). Comparison of different efficiency criteria for hydrological model. *Advances in Geosciences, 5*, 89-97.

Monetary Authority of Singapore. (2019, Nov). Exchange Rates. Singapore, Singapore. Retrieved Nov 2019, from https://secure.mas.gov.sg/msb/ExchangeRates.aspx

Mughal, M., Li, X.-X., Yin, T., Martilli, A., Brousse, O., Dissegna, M., & Norford, L. (2019). High-Resolution , Multilayer Modeling of Singapore's Urban Climate Incorporating Local Climate Zones. *Journal of Geophysical Research: Atmospheres, 124*(14), 1-22.

Nag, P. K. (2002). *Power Plant Engineering.* Tata McGraw-Hill Education.

National Environment Agency. (2020, January). *Refuse Disposal Facility*. Retrieved from National Environment Agency Official Website: https://www.nea.gov.sg/our-

services/waste-management/3r-programmes-and-resources/waste-management-infrastructure/refuse-disposal-facility

NIST/SEMATECH. (2013, Oct). Engineering Statistics Handbook. USA. Retrieved Feb 18, 2020, from https://www.itl.nist.gov/div898/handbook/apr/apr.htm

Noordermeer, J. (n.d.). *ogeneration and Combined-Cycle Principles Workshop© by Jim Noordermeer (Former Employee).* Retrieved from CHA Canada: http://www.chacanada.com/news/white-papers/cogeneration-and-combined-cycle-principles-workshop/

PA Consulting Group. (2018). *Review of the Vesting Contract Technical Parameters for the period 1 January 2019 to 31 December 2020.* Singapore: Energy Market Authority. Retrieved 2019, from https://www.ema.gov.sg/cmsmedia/Annex%202_Review%20of%20the%20Vesting%20Contract%20Technical%20Parameters_Final__.pdf

Pacific Northwest National Laboratory. (n.d.). *Lower and Higher Heating Values of Fuels*. Retrieved from Hydorgen Tools: https://h2tools.org/hyarc/calculator-tools/lower-and-higher-heating-values-fuels

SP Group. (2017). *Electricity Cable Tunnel Projects*. Retrieved Dec 2019, from SP Group Corporate Web Site: https://www.spgroup.com.sg/cable-tunnel/home.html

Strbac, G., & Aunedi, M. (2016). *Whole-system cost of variable renewables in future GB electricity system.* London: Imperial College London. doi:10.13140/RG.2.2.24965.55523

Suresh, M. V., Reddy, K. S., & Kolar, A. K. (2012). Thermodynamic analysis of a coal-fired power plant repowered with pressurized pulverized coal combustion. *Proceedings of the Institution of Mechanical Engineers, Part A: Journal of Power and Energy, 226*(1), 5-16.

Thorin, E., Sandberg, J., & Yan, J. (2015). Combined Heat and Power. In J. Yan, *Handbook of Clean Energy Systems* (pp. 1185-1188). New York: John Wiley & Sons.

US Energy Information Administration. (2019, Mar). Table 8.2. Average Tested Heat Rates by Prime Mover and Energy Source, 2008-2018. Washington, DC, Virginia, United States of America. Retrieved Jan 2020

US Energy Information Administration. (2020, Feb). *Natural Gas.* Retrieved from US Energy Information Administration: https://www.eia.gov/dnav/ng/hist/rngwhhdD.htm

Wärtsilä. (2020). *Combustion Engine vs. Gas Turbine: Part Load Efficiency and Flexibility*. Retrieved from Wärtsilä corporate site: https://www.wartsila.com/energy/learn-more/technical-comparisons/combustion-engine-vs-gas-turbine-part-load-efficiency-and-flexibility

World Bank Group. (2019, Dec). *Commodity Markets.* (B. P. Dow, Ed.) Retrieved from World Bank Group: https://www.worldbank.org/en/research/commodity-markets#1

Annex A – Power plant database

Table A1. *Main power plant data*

ID	Power Plant	Owner/Operator	Year	Registered Capacity [MW]	Technology	Fuel	Fuel ID*	Cooling System	Stack height [m]	Condenser exhaust height [m]	Unit Name	lat (°)	long (°)
0	Senoko Power Station	Senoko Energy Pte Ltd	2012	862	CCGT	nat gas	LNG (JKM)	once-through	100	0	SNK CCP 6, 7	1.46	103.80
1	Senoko Power Station	Senoko Energy Pte Ltd	2004	730	CCGT	nat gas	PNG (HH)	once-through	100	0	SNK CCP 4, 5	1.46	103.80
2	Senoko Power Station	Senoko Energy Pte Ltd	2002	365	CCGT	nat gas	PNG (HH)	once-through	100	0	SNK CCP 3	1.46	103.80
3	Senoko Power Station	Senoko Energy Pte Ltd	1996	850	CCGT	nat gas	PNG (HH)	once-through	100	0	SNK CCP 1, 2	1.46	103.80
4	Senoko Power Station	Senoko Energy Pte Ltd		493	Oil-fired ST	crude oil	Crude (Dubai)	once-through	100	0	SNK OilST	1.46	103.80
5	Pulau Seraya Power Station	YTL PowerSeraya Pte Ltd	2010	740	Cogen CCGT	nat gas	LNG (JKM)	BP-cogen	100		PulSer CCP3, 4	1.28	103.73
6	Pulau Seraya Power Station	YTL PowerSeraya Pte Ltd	2002	732	CCGT	nat gas	PNG (HH)	once-through	100	0	PulSer CCP1, 2	1.28	103.73
7	Pulau Seraya Power Station	YTL PowerSeraya Pte Ltd		724	Oil-fired ST	Orimulsion	Crude (Dubai)	once-through	100	0	PulSer OilST1	1.28	103.73
8	Pulau Seraya Power Station	YTL PowerSeraya Pte Ltd		724	Oil-fired ST	heavy fuel oil	Crude (Brent)	once-through	100	0	PulSer OilST2	1.28	103.73
9	Jurong Power Station	YTL PowerSeraya Pte Ltd		180	OCGT	diesel	Crude (WTI)	once-through	100	0	JRNG OCGT	1.31	103.71
10	Tuas Power Station	Tuas Power Generation Pte Ltd	2014	406	Cogen CCGT	nat gas	LNG (JKM)	BP-cogen	100		TUACCP5	1.29	103.64
11	Tuas Power Station	Tuas Power Generation Pte Ltd	2005	735	CCGT	nat gas	PNG (HH)	once-through	100	0	TUACCP3, 4	1.29	103.64
12	Tuas Power Station	Tuas Power Generation Pte Ltd	2002	735	CCGT	nat gas	PNG (HH)	once-through	100	0	TUACCP1, 2	1.29	103.64

ID	Power Plant	Owner/Operator	Year	Registered Capacity [MW]	Technology	Fuel	Fuel ID*	Cooling System	Stack height [m]	Condenser exhaust height [m]	Unit Name	lat (°)	long (°)
13	Tuas Power Station	Tuas Power Generation Pte Ltd		600	Oil-fired ST	oil	Crude (Dubai)	once-through	100	0	TUA OilST	1.29	103.64
14	Sembcorp Cogen @ Banyan	SembCorp Cogen Pte Ltd	2014	404	Cogen CCGT	nat gas	LNG (JKM)	BP-cogen	100		SKACCP3	1.26	103.67
15	Pulau Sakra Power Station	SembCorp Cogen Pte Ltd	2001	785	Cogen CCGT	nat gas	PNG (HH)	BP-cogen	100		1.255752	1.26	103.7
16	Keppel Merlimau Cogen Power Station	Keppel Merlimau Cogen Pte Ltd	2013	840	Cogen CCGT	nat gas	LNG (JKM)	BP-cogen	100		KepMer CCP2	1.28	103.68
17	Keppel Merlimau Cogen Power Station	Keppel Merlimau Cogen Pte Ltd	2007	470	Cogen CCGT	nat gas	PNG (HH)	BP-cogen	100		KepMer CCP1	1.28	103.68
18	PacificLight Power Plant	PacificLight Power Pte Ltd	2014	800	CCGT	nat gas	LNG (JKM)	once-through	100	0	PLP Unit 1, 2	1.28	103.72
19	Tuaspring Integrated Water & Power Project	Tuaspring Plant Pte Ltd	2016	396	CCGT	nat gas	LNG (JKM)	once-through	100	0	TI CCP	1.30	103.62
20	Tuas South Incineration Plant	National Environment Agency	2000	131	WtE ST	waste		dry-cooling	150	10	TSIP WtE	1.30	103.62
21	Tuas Incineration Plant	National Environment Agency	1986	49.8	WtE ST	waste		dry-cooling	150	10	TIP WtE	1.33	103.63
22	Senoko Waste-to-Energy Plant	Senoko WTE Pte Ltd	1992	55	WtE ST	waste		dry-cooling	150	10	SNK WtE	1.46	103.79

ID	Power Plant	Owner/Operator	Year	Registered Capacity [MW]	Technology	Fuel	Fuel ID*	Cooling System	Stack height [m]	Condenser exhaust height [m]	Unit Name	lat (°)	long (°)
23	Keppel Seghers Tuas Waste-to-Energy Plant	Keppel Seghers Tuas WTE Pte Ltd	2009	22	WtE ST	waste		dry-cooling	100	10	KepSeg WtE	1.30	103.62
24	Tembusu BMCC Plant	TP Utilities Pte Ltd	2013	160	Cogen Extraction ST	clean coal, biomass, nat gas	Coal (AU)	once-through	100	0	TMUC CCP	1.27	103.68
25	ExxonMobil Cogen Plant	ExxonMobil Asia Pacific Pte Ltd	2012	332	Cogen CCGT	nat gas	LNG (JKM)	BP-cogen	100		ExxMob CCP	1.28	103.70

Table A2. *Technical parameters*

ID	Unit Name	Full Load Efficiency [%]	Efficiency rand var*	Efficiency Curve*	Cogen Total Efficiency	Min Stable Generation [MW]	Average Failures per year [yr-1]	Mean Time to Repair [wks]	MTTF [wks]	Alim [-]
0	SNK CCP 6, 7	48.8	eff_skewed	CCGT GT26		431	10.44	0.63	4.37	0.87
1	SNK CCP 4, 5	62.3	eff_skewed	CCGT Best		365	22.54	0.45	1.87	0.81
2	SNK CCP 3	58.4	eff_skewed	CCGT Best		183	4.69	1.57	9.54	0.86
3	SNK CCP 1, 2	60.4	eff_skewed	CCGT Best		425	9.44	0.64	4.88	0.88
4	SNK OilST	37.1	eff_skewed	ST sample		247	6.09	0.68	7.89	0.92
5	PulSer CCP3, 4	35.1	eff_skewed	CCGT Typical	83.0	370	14.07	0.40	3.31	0.89
6	PulSer CCP1, 2	62.5	eff_skewed	CCGT GT26		366	5.92	0.38	8.43	0.96
7	PulSer OilST1	34.2	eff_skewed	ST sample		362	13.40	0.64	3.25	0.83
8	PulSer OilST2	34.0	eff_skewed	ST sample		362	9.41	0.81	4.73	0.85
9	JRNG OCGT	36.4	eff_skewed	CCGT Typical		90	10.53	0.28	4.68	0.94
10	TUACCP5	38.4	eff_skewed	CCGT 4000F	83.0	203	5.47	0.38	9.16	0.96
11	TUACCP3, 4	61.8	eff_skewed	CCGT Typical		368	8.69	0.56	5.44	0.91
12	TUACCP1, 2	61.2	eff_skewed	CCGT Typical		368	2.98	3.49	14.00	0.80

ID	Unit Name	Full Load Efficiency [%]	Efficiency rand var*	Efficiency Curve*	Cogen Total Efficiency	Min Stable Generation [MW]	Average Failures per year [yr-1]	Mean Time to Repair [wks]	MTTF [wks]	Alim [-]
13	TUA OilST	35.4	eff_skewed	ST sample		300	21.07	0.25	2.23	0.90
14	SKACCP3	34.2	eff_skewed	CCGT 9F.05	83.0	202	4.96	1.07	9.43	0.90
15	SKACCP1, SKACCP2	39.8	eff_skewed	CCGT Typical	83.0	393	22.63	0.39	1.92	0.83
16	KepMer CCP2	39.2	eff_skewed	CCGT GT26	83.0	420	7.06	1.08	6.31	0.85
17	KepMer CCP1	36.8	eff_skewed	CCGT 4000F	83.0	235	14.82	0.35	3.17	0.90
18	PLP Unit 1, 2	59.9	eff_skewed	CCGT 701F		400	22.96	0.32	1.95	0.86
19	TI CCP	61.1	eff_skewed	CCGT 701F		198	18.93	0.19	2.56	0.93
20	TSIP WtE	21.8	eff_skewed	ST sample		66	15.99	0.42	2.84	0.87
21	TIP WtE	18.1	eff_skewed	ST sample		25	12.97	0.47	3.54	0.88
22	SNK WtE	23.1	eff_skewed	ST sample		28	2.28	3.85	19.03	0.83
23	KepSeg WtE	20.0	eff_skewed	ST sample		11	13.12	0.34	3.63	0.91
24	TMUC CCP	40.0	eff_skewed	ST sample	80.0	80	7.07	0.99	6.38	0.87
25	ExxMob CCP	35.7	eff_skewed	CCGT GT26	83.0	166	12.97	0.79	3.23	0.80

Table A3. *Random Seeds*

ID	Power Plant	Unit Name	Full Load Efficiency	Start Online	UP Time Duration	DOWN Time Duration
0	Senoko Power Station	SNK CCP 6, 7	209652396	398764591	924231285	1478610112
1	Senoko Power Station	SNK CCP 4, 5	441365315	1537364731	192771779	1491434855
2	Senoko Power Station	SNK CCP 3	1819583497	530702035	626610453	1650906866
3	Senoko Power Station	SNK CCP 1, 2	1879422756	1277901399	1682652230	243580376
4	Senoko Power Station	SNK OilST	1991416408	1171049868	1646868794	2051556033
5	Pulau Seraya Power Station	PulSer CCP3, 4	1252949478	1340754471	124102743	2061486254

ID	Power Plant	Unit Name	Full Load Efficiency	Start Online	UP Time Duration	DOWN Time Duration
6	Pulau Seraya Power Station	PulSer CCP1, 2	292249176	1686997841	1827923621	1443447321
7	Pulau Seraya Power Station	PulSer OilST1	305097549	1449105480	374217481	636393364
8	Pulau Seraya Power Station	PulSer OilST2	86837363	1581585360	1428591347	1963466437
9	Jurong Power Station	JRNG OCGT	1194674174	602801999	1589190063	1589512640
10	Tuas Power Station	TUACCP5	2055650130	2034131043	1284876248	1292401841
11	Tuas Power Station	TUACCP3, 4	1982038771	87950109	1204863635	768281747
12	Tuas Power Station	TUACCP1, 2	507984782	947610023	600956192	352272321
13	Tuas Power Station	TUA OilST	615697673	160516793	1909838463	1110745632
14	Sembcorp Cogen @ Banyan	SKACCP3	93837855	454869706	1780959476	2034098327
15	Pulau Sakra Power Station	SKACCP1, SKACCP2	1136257699	800291326	1177824715	1017555826
16	Keppel Merlimau Cogen Power Station	KepMer CCP2	1959150775	930076700	293921570	580757632
17	Keppel Merlimau Cogen Power Station	KepMer CCP1	80701568	1392175012	505240629	642848645
18	PacificLight Power Plant	PLP Unit 1, 2	481447462	954863080	502227700	1659957521
19	Tuaspring Integrated Water & Power Project	TI CCP	1905883471	1729147268	780912233	1932520490
20	Tuas South Incineration Plant	TSIP WtE	1544074682	485603871	1877037944	1728073985
21	Tuas Incineration Plant	TIP WtE	848819521	426405863	258666409	2017814585
22	Senoko Waste-to-Energy Plant	SNK WtE	716257571	657731430	732884087	734051083
23	Keppel Seghers Tuas Waste-to-Energy Plant	KepSeg WtE	903586222	1538251858	553734235	1076688768
24	Tembusu BMCC Plant	TMUC CCP	1354754446	463129187	1562125877	1396067212
25	ExxonMobil Cogen Plant	ExxMob CCP	301492857	165035946	1883779156	576702667